Defence Research and Development Canada
Recherche et développement pour la défense Canada

DEFENCE R&D DÉFENSE

# Active polarimetric imaging of solid targets

*Depolarization and reflectivity analysis*

*Xiaoying Cao*

*Prepared by:*

*AEREX avionique inc.*
*324, St-Augustin Ave.*
*Breakeyville (Quebec)*
*G0S 1E1*

*Project Manager: Daniel Pomerleau, 418- 832-1040*
*Contrat Number: W7701-072533*
*Contract Scientific Authority: Gilles Roy, 418 844 4000 (4335)*



**Defence R&D Canada – Valcartier**
Contract Report
DRDC Valcartier CR 2010-362
November 2010

Canada

# Active polarimetric imaging of solid targets

*Depolarization and reflectivity analysis*

Xiaoying Cao

Prepared by:
AEREX avionique inc.
324, St-Augustin Ave.
Breakeyville (Quebec)
G0S 1E1

Project Manager: Daniel Pomerleau, 418- 832-1040

Contractor number: W7701-072533

Contract Scientific Authority: Gilles Roy, 418 844 4000 (4335)



**Defence R&D Canada – Valcartier**

**Contract Report**

DRDC Valcartier CR 2010-362

November 2010

Author 

Xiaoying Cao

Approved by 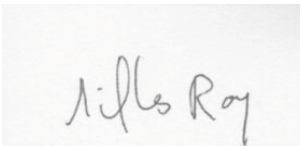

Gilles Roy

Defense scientist

Work performed under: ARP 15dk: Current and Emerging Image Exploitation Techniques

# Abstract

Measurements of solid targets depolarization and reflectivity signatures were performed using a polarization imaging lidar. The lidar consists of a Q-switched laser operating at 532 nm, a telescope and a gated intensified CCD camera from Andor. Over 70 different materials have been examined. The different materials consist of different insulation materials, woods, metals, sand papers, concrete, wet/dry sands and environmental targets. Four incident angles measurements were conducted to examine the influence of light incident angle on the targets depolarization signature and reflectivity. The main observations are: (1) Metal targets show little depolarization but large reflectivity for incidence angle close to $0^o$; their reflectivity drops rapidly with an increase of the incident angle while depolarization increases. (2) Randomly oriented materials targets with high reflectivity show high depolarization ratio, and low reflectivity are associated with low depolarization ratio. Their depolarization ratios are almost not dependent on the light incident angle. (3) The circular depolarization ratios are typically 2 to 3 time larger than the linear depolarization ratios.



# Résumé

Les signatures en polarisations et en intensité de cibles ont été mesurées à l'aide d'un lidar polarisant imageant. Le lidar consiste en un laser 'Q switch' opérant à 532nm, un télescope et une caméra intensifiée à crénelage temporel fabriquée par Andor. Plus de 70 matériaux différents ont été évalués. Les différentes cibles consistent en différents matériaux d'isolation, bois, métaux, papiers sablés, ciment, sable sec/mouillé et d'autres cibles de type environnemental. Quatre angles d'incidences ont été utilisés pour étudier l'influence de l'angle d'incidence sur les signatures en polarisation et réflectivité. Les observations principales sont : (1) les cibles métalliques dépolarisent faiblement la lumière et ont une réflectivité élevée pour des angles d'incidences près de $0^o$ ; la réflectivité diminue rapidement avec une augmentation de l'angle d'incidence, alors que le ratio de dépolarisation augmente. (2) Les cibles constituées de matériaux distribués aléatoirement qui ont une haute réflectivité présente des ratios de dépolarisation élevés; Les cibles constituées de matériaux distribués aléatoirement qui ont une faible réflectivité présentent des ratios de dépolarisation faibles. (3) Les ratios de dépolarisation circulaires sont 2 à 3 fois plus élevés que les ratios de dépolarisation linéaires.

This page intentionally left blank.

# Executive summary

**Active polarimetric imaging of solid targets: depolarization and reflectivity analysis**

**Introduction or background:** Defence Research & Development Canada –Valcartier initiated many projects on polarization lidar for laser atmospheric propagation studies in clouds. The same technology further developed can be applied to the study of solid objects depolarization and scattered light intensity. The leading idea is to determine the discrimination capability of the polarization and intensity signatures from different objects/targets.

**Results:** Measurements of solid targets depolarization and reflectivity signatures were performed using a polarization imaging lidar. The lidar consists of a Q-switched laser operating at 532 nm, a telescope and a gated intensified CCD camera from Andor. Over 70 different materials have been evaluated. The different targets consist of different insulation materials, woods, metals, sand papers, concrete, wet/dry sands and environmental target. Four incident angles measurements were conducted to examine the influence of light incident angle on the targets depolarization signature and reflectivity. The main observations are: - Metal targets show little depolarization but large reflectivity for incidence angle close to $0^{o}$; their reflectivity drops rapidly with an increase of the incident angle while their depolarization increases. - Randomly oriented materials targets with high reflectivity show high depolarization ratios are almost independent on the light incident angle. -Randomly oriented materials with low reflectivity show low depolarization ratios almost independent of the light incident angle. The circular depolarization ratios are typically 2 to 3 times larger than the linear depolarization ratios.

**Significance:** Preliminary results indicate that discrimination of materials based on depolarization and intensity signatures appears possible. This could lead to better recognition and identification of targets.

**Future plans:** Measurements performed under better control environment is required to better assess the level of discrimination that could be obtained between the different materials.

Cao X. 2010, CR 2010-999. Defence R&D Canada – Valcartier; September 2010.

# Sommaire

## Polarimétrie imageante active de cibles solides : analyse de la dépolarisation et de la réflectivité

**Introduction ou contexte:** Recherche et Développement Canada-Valcartier (RDDC Valcartier) a initié plusieurs projets portant sur l'utilisation des lidar polarisants pour effectuer des travaux sur la propagation des lasers à travers les nuages. La même technologie développée peut-être appliquée à l'étude de la signature en dépolarisation et en intensité d'objet solide. L'idée maitresse est de déterminer la capacité discriminante des signatures en polarimétrie et en intensité de différents objets/cibles.

**Résultats:** Les signatures en polarisations et en intensité de cibles ont été mesurées à l'aide d'un lidar polarisant imageant. Le lidar consiste en un laser 'Q switch' opérant à 532nm, un télescope et une caméra intensifiée à crénelage temporel fabriquée par Andor. Plus de 70 matériaux différents ont été évalués. Les différents matériaux consistent en différents matériaux d'isolation, bois, métaux, papiers sablés, ciment, sable sec/mouillé et d'autre cibles de type environnemental. Quatre angles d'incidence ont été utilisés pour étudier l'influence de l'angle d'incidence sur les signatures en polarisation et réflectivité. Les observations principales sont : les cibles métalliques dépolarisent faiblement la lumière et ont une réflectivité élevée pour des angles d'incidence près de $0^o$ ; la réflectivité diminue rapidement avec une augmentation de l'angle d'incidence, alors que le ratio de dépolarisation augmente. - Les cibles constituées de matériaux distribués aléatoirement qui ont une haute réflectivité présentent des ratios de dépolarisation élevés. - Les cibles constituées de matériaux distribués aléatoirement qui ont une faible réflectivité présentent des ratios de dépolarisation faibles. Les ratios de dépolarisation circulaires sont 2 à 3 fois plus élevés que les ratios de dépolarisation linéaires.

**Importance:** Les résultats indiquent que la discrimination de matériaux apparaît, dans une certaine mesure, possible à partir de leurs signatures en polarisation et en intensité

**Perspectives:** Des mesures effectuées dans des conditions mieux contrôlées sont requises pour mieux déterminer le degré de discrimination que l'on peut obtenir entre les différents matériaux

Cao X. 2010, CR 2010-362 Defence R&D Canada – Valcartier; September 2010

# Table of contents

# List of figures

# List of tables

**This page intentionally left blank.**

# 1. Introduction

Defence Research & Development Canada –Valcartier initiated many projects on polarization lidar for laser atmospheric propagation studies in clouds. The same technology further developed is applied to the study of solid objects depolarization and scattered light intensity. The leading idea is to determine the discrimination capability of the polarization and intensity signatures for different objects/targets.

To do so, measurements of solid targets depolarization and reflectivity signatures were performed using a polarization imaging lidar. Over 70 different targets have been evaluated. The different materials consist of different insulation materials, woods, metals, sand papers, concrete, wet/dry sands and environmental targets.

The report is divided into 7 parts. It starts with the introduction of the project, and the objective, followed by description of field experiment set up for wavelength of 532 nm. The third part is the data process procedure, mainly for data obtained from dual-polarized imaging lidar operated at 532 nm. The different materials were glued on panels and the corresponding analysis results and findings for each panel are discussed in the fourth part. In the fifth part, analysis results from dual-polarized lidar operated at 1570 nm are discussed. The comparison of targets depolarization between two wavelengths is described in part 6. The last part is the conclusion and discussion.

# 2. Experimental Set-up

Figure 1a shows the general layout of RDDC Valcartier aerosol chamber and lidar measurement facility. The different targets were mounted at the back of the aerosol chamber at a distance of 121 m from the lidar to prevent effect of outside elements.

The measurements were performed using the RDDC-Valcartier 532-nm dual polarization imaging MFOV lidar, see Ref. [1]. It consists of a telescope coupled to a gated intensified CCD camera (G-ICCD) synchronized with a doubled Nd-YAG laser. The laser beam is pointed at the desired location using a scene mirror and a scanner. The analyzer consists of two polarized cube beam splitters and a single ICCD camera used to image simultaneously the two polarization states of the backscattered polarization, as shown in Figure 1b. At the emission, a vertical linear polarization can be changed to a horizontal polarization using a $\lambda/2$ wave plate and to a circular right or left polarization using a $\lambda/4$ wave plate.

When the polarized laser beam from the lidar hits the target, part of the light is absorbed while the other part is reflected. The back-reflected light with its two polarization components (parallel (p) and orthogonal (s)) were collected and imaged side by side on a ICCD camera. Attenuators were set in front of the ICCD camera to attenuate signal intensity to avoid the CCD chip of the camera being saturated. The back-reflected light passed through a quarter-wave plate before the signal arrived to the camera. The fast axis of the wave plate was set at 0° for linearly polarized light, and at 45° for circularly polarized light to make sure the light that reached the camera was linearly polarized. Details of wave plates settings can be found in Ref. [1].

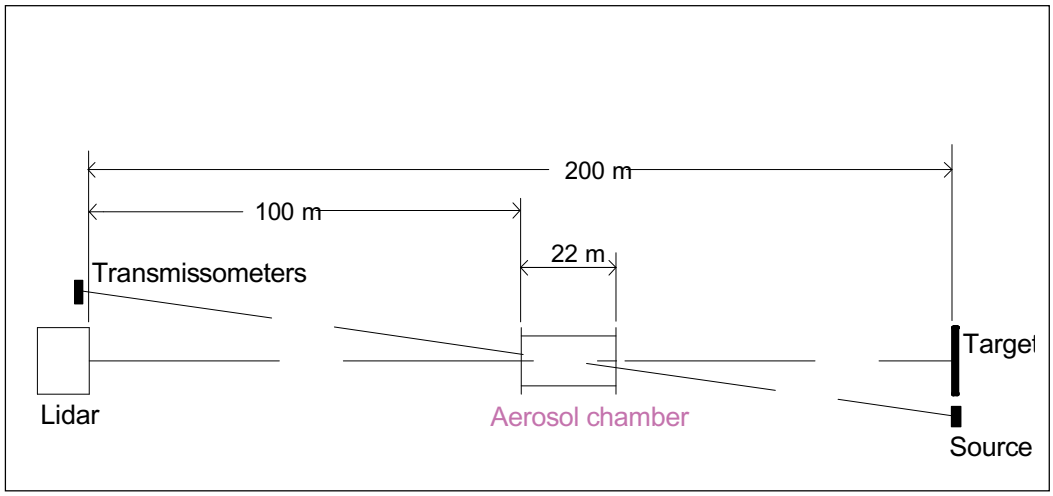


***Figure 1a.*** *General layout of RDDC Valcartier aerosol chamber and lidar measurement facility. The different targets were mounted at the back of the aerosol*

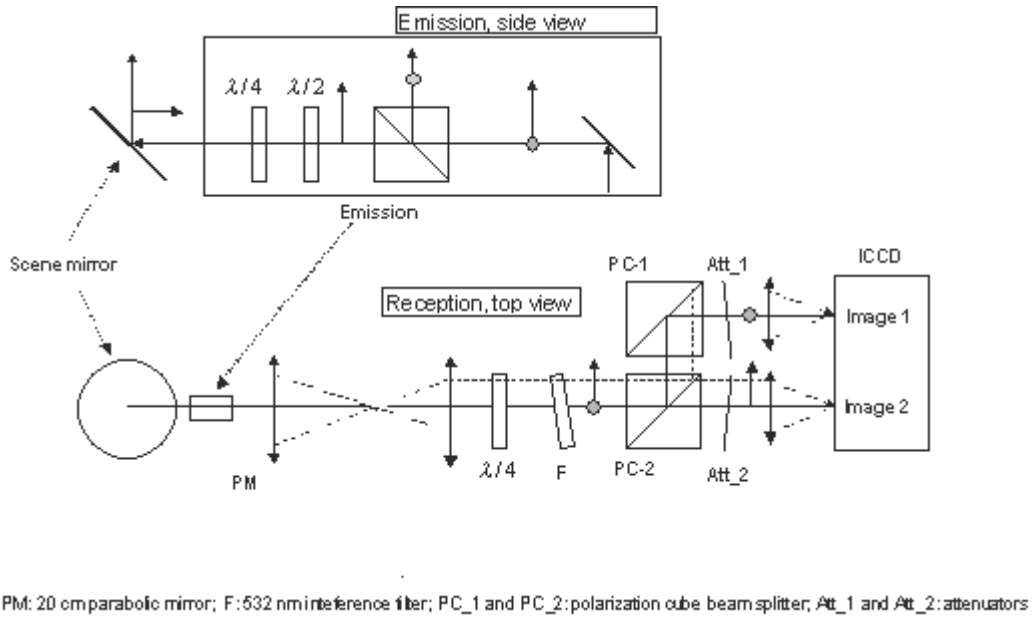


***Figure 1b.*** *Schematic illustration of the MFOV lidar*


***Figure 1c****. For each panel type there is three permanent targets always on the top of the board. They are: black board (#1), 99% reflectivity Spectralon (#2) and 2% reflectivity Spectralon #3). The dimensions of the Spectralons are 12cm x 12cm and the other subtargets 10cm x 10cm.*

In order to illuminate the target, the laser beam divergence was increased using a lens external to the system. To examine the influence of incidence angle on target depolarization ratio and reflectivity, panels were set up and measured at desired angles. Targets made of different materials were examined, including insulations, woods, metals, sand papers, concrete, grasses, wet and dry sands, as well as other environmental targets with each material category (panel) containing some subtargets. Subtargets of each target category were glued on a black wooden board and the board was set up at the end of a chamber. Figure 1c illustrates a typical target and subtargets assembly. The target shown is 90° rotated toward right. For each panel type, there were three permanent targets always on the top of the board. They are: black board (#1), 99% reflectivity Spectralon (#2) and 2% reflectivity Spectralon (#3). To give an idea of the dimensions, the spectralons are 12cm x 12cm and the other subtargets 10cm x 10cm. So at a distance of 120m, the Spectralons cover a FOV of 1 mrad.

# 3. Data process

The precise measurement of the depolarization ratio requires the knowledge of the relative response of both polarization channels, Ref [1]. Moreover, the analysis of relative reflectivity should be based on uniform laser beam illumination. Therefore, signal calibration is necessary before further analysis.

## 3.1 Relative system calibration

The lidar measurements need to be calibrated to take into account the relative responses of the two polarization channels which are affected by: the attenuator transmission values, the mirror reflectivity difference between the s and p waves, and signal losses in the cubes. Relative calibration (calibration to measurements of left image) of the lidar system should be performed to ensure both linear (linear vertical and horizontal) or circular (circular right and left) depolarizations obtained are the same (ideally) or close enough (in reality). We used the same calibration procedure as introduced by Roy and Roy (2008), Ref [2].

The relative calibration factors were calculated based on the measurements of a homogeneous target with low depolarization. The target depolarization ratio is intrinsic to the material nature and does not depend on the polarization 'orientation' (linear vertical/ horizontal or circular left /right) of the incident radiation. After calibration, depolarization ratios as results of linear vertically polarized light and circular polarized light can be compared for different targets.

## 3.2 Laser beam uniformity calibration

In order to illuminate most of the panel targets, a large beam divergence was used. The intensity of the laser beam is not uniformly distributed. To examine the reflectivity of each target, the non-uniformity of the laser beam has to be estimated. This is called laser-beam uniformity calibration.

The laser beam illumination measurement was done using a homogeneous target; we have used the supporting black painted wooden board. For each polarized (linear horizontal and vertical, circular right and left) light, 5 individual measurements of the homogeneous target were averaged, and the maximum value of the average of the right (image) was used as the reference to calibrate the other pixels of the image. The same procedure was applied to the left (image). The generated calibration matrix was applied to each target category. To make it clear, an example follows:

Assume the left and right image matrices of the uniform target after 5 measurements averaging are $M_L$ and $M_R$ with pixel elements $m_{Lij}$ and $m_{Rij}$. The largest elements of the $M_L$ and $M_R$ are $m_L$ and $m_R$. Then, the calibration matrices for left and right images are:

$$C_L = M_L./m_L = \{c_{Lij}\} = \{m_{Lij}/m_L\}. \quad (1)$$

and

$$C_R = M_R./m_R = \{c_{Rij}\} = \{m_{Rij}/m_R\}. \quad (2)$$

If the matrices of left and right images of the measured target are $T_L$ and $T_R$ respectively, then after laser beam uniformity calibration, the calibrated image matrices will be:

$$T_{L\_C} = C_L \cdot \times T_L = \{c_{Lij} \cdot t_{Lij}\}. \quad (3)$$

and

$$T_{R\_C} = C_R \cdot \times T_R = \{c_{Rij} \cdot t_{Rij}\}. \quad (4)$$

Figure 2 shows a comparison of image intensity of a uniform target of the black wooden board before and after uniformity calibration. Obviously, after calibration, the light intensity distribution on the homogeneous target is more uniform than the one without calibration. Figure 3 shows images of subtargets on a panel before and after the uniformity calibration. From figure 3, one can see that, before the calibration, the lidar detected more energy from the second row targets, while after calibration, the left bottom target was found to have reflected more energy.

## 3.3 Depolarization ratio and reflectivity

Depolarization ratios (δ) of targets were calculated after system calibration and uniformity calibration, i.e.

$$\delta = \frac{I_\perp}{I_{//}}. \quad (5)$$

where, $I_\perp$ is the intensity received in the secondary polarization channel, and $I_{//}$ is the intensity of the principal polarization. The ICCD camera can record image of matrix size 1024*256 (pixels). However, it was found that only the central 691 columns are properly

amplified. During the measurement, the camera system was set up to record the signals of column from 167 to 857, resulting in the matrix size of 691*256. The panel matrix is composed of a number of sub-matrices representing the subtargets. The sub-matrix is corresponding to each subtarget and its location in the panel needs to be specified before calculation. This is done by recording the position of each subtarget Andor camera images, as shown in Figure 4.

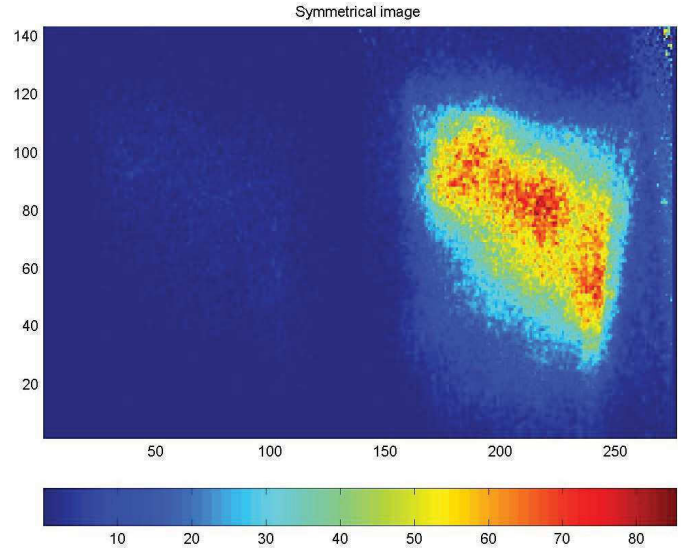


(a)

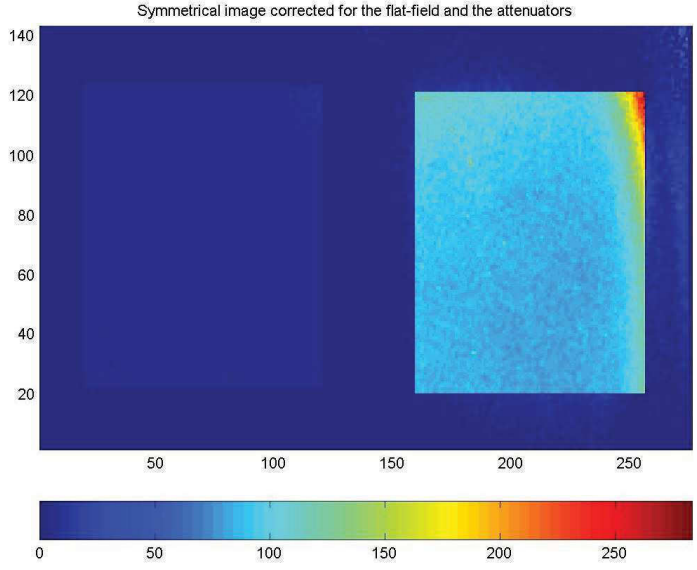


(b)

***Figure 2.*** *Images of uniform target before (a) and after (b).uniformity calibration*

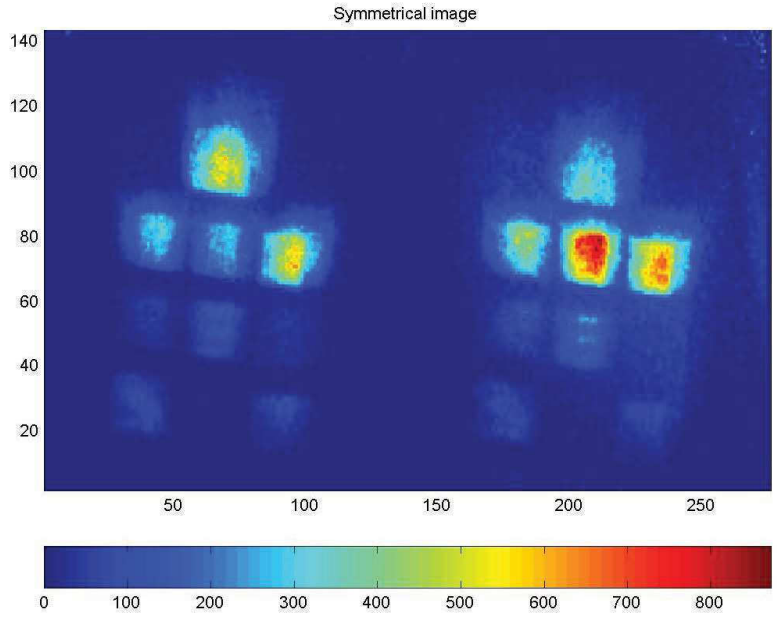


(a)

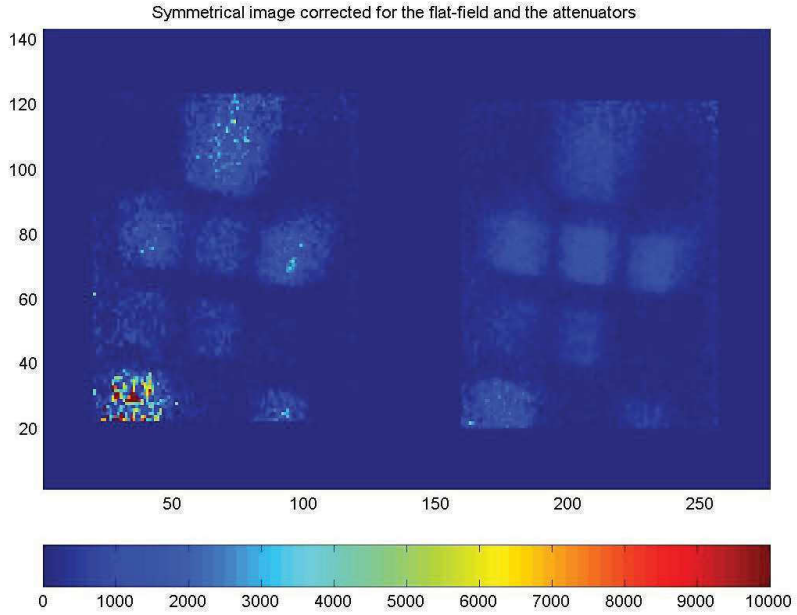


(b)

***Figure 3.*** *Images of targets on a panel before (a) and after (b).uniformity calibration*

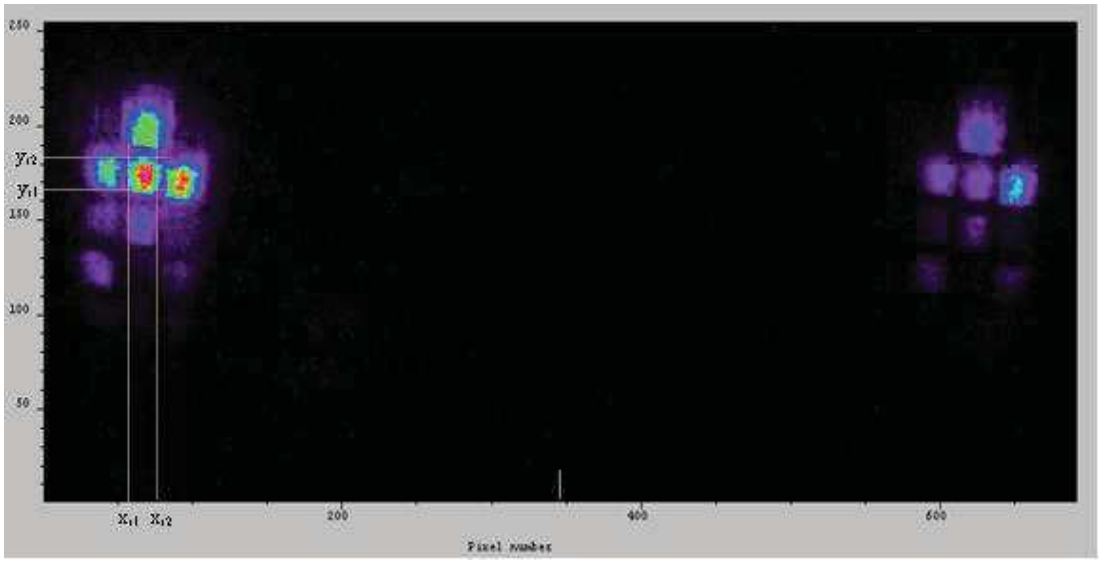


***Figure 4**. Locate subtarget from the ICCD image*

To reduce the influence of non-perfect uniformity calibration on the depolarization, the pixel average intensity of each subtarget was used for the computation of depolarization ratio and reflectivity.

$$\delta_k = \frac{\sum_{i,j} I_{\perp}(i,j) \Big/ n_{k\perp}}{\sum_{m,n} I_{//}(m,n) \Big/ n_{k//}}. \tag{6}$$

where, $i = i_1, \cdots, i_p$, $j = j_1, \cdots, j_q$, $m = m_1, \cdots, m_s$, $n = n_1, \cdots, n_t$, with $1 \le i, m \le 691$, $1 \le j, n \le 256$, and $n_{k\perp}$ and $n_{k//}$ are the total pixel numbers covered by the subtarget image k corresponding to the s and p components, respectively.

For convenience, relative reflectivity ($R$) will be used, i.e., the ratio of pixel-averaged energy received from target 'k' to the energy from the target of 99% reflectivity Spectralon. Thus, the relative reflectivity is the reflectivity relative to the 99% Spectralon at each incident angle.

$$R_k = \frac{I_k(tot)}{I_{ref}(tot)} = \frac{I_{k\perp}(tot)/n_{k\perp} + I_{k//}(tot)/n_{k//}}{I_{ref\perp}(tot)/n_{ref\perp} + I_{ref//}(tot)/n_{ref//}}. \tag{7}$$

where $I(tot)$ is the total energy of unit pixel cell from both p and s channels. $k$ represents subtarget $k$, and ref represents reference target, here the 99% reflectivity Spectralon.

# 4. Experimental results

Different targets made of different materials were examined; they are categorized as insulations, woods, metals, sand papers, concrete, grasses, wet/dry sands and environmental targets. These targets will be analyzed and discussed one by one by their category. As explained previously, on each panel type, there are three permanent targets always on the top of the board. They are black board, 99% reflectivity Spectralon and 2% reflectivity Spectralon.

## 4.1 Panel 1 – Insulations

Panel 1 consists of insulation targets. Figure 5 and table 1 provide the relevant information. Figure 5 is the picture of insulation targets. From now on, all subtargets will be cited by target number shown on each board.


***Figure 5.*** *Picture of insulation targets on panel 1*

***Table 1.*** *List of targets on panel 1*

| **Panel 1- Insulation** |
|---|
| 1. black wood |
| 2. 99% spectralon |
| 3. 2% spectralon |
| 4. Blue extruded polystyrene (StyrofoamØ ) |
| 5. Pink extruded polystyrene (StyrofoamØ ) |
| 6. White extruded polystyrene (StyrofoamØ ) |
| 7. polyurethane foam insulation |
| 8. White styro foam |
| 9. black styro foam |
| 10. ReflectikØ |
| 11. Black light Styrofoam |
| 12. Beige Styrofoam |
| 13. Transparent mini-bubble |
| 14. FireProof wool |
| 15. Horizontal Mineral wool |

Table 2 lists the depolarization ratio analysis results of targets on panel 1. It is found that circular depolarization ratio $\delta_C$ is about twice the value of $\delta_L$ for almost all targets. The influence of incident angle on depolarizations can be easily seen from Figure 6 and Table 2.

***Table 2.*** *Depolarization ratios of targets on panel 1at different incident angle*

| Taget # | Depolarization ratio | | | | | | | |
|---|---|---|---|---|---|---|---|---|
| | $\delta_L$ | | | | $\delta_C$ | | | |
| | 0° | 15° | 30° | 45° | 0° | 15° | 30° | 45° |
| 1 | 0.10 | 0.12 | 0.14 | 0.16 | 0.27 | 0.32 | 0.36 | 0.43 |
| 2 | 0.44 | 0.51 | 0.47 | 0.50 | 1.27 | 1.49 | 1.43 | 1.58 |
| 3 | 0.17 | 0.31 | 0.24 | 0.24 | 0.40 | 0.73 | 0.59 | 0.68 |
| 4 | 0.41 | 0.46 | 0.53 | 0.58 | 0.73 | 0.83 | 0.91 | 1.07 |
| 5 | 0.23 | 0.26 | 0.36 | 0.41 | 0.36 | 0.44 | 0.65 | 0.82 |
| 6 | 0.59 | 0.46 | 0.48 | 0.54 | 0.88 | 0.70 | 0.73 | 0.91 |
| 7 | 0.30 | 0.37 | 0.36 | 0.32 | 0.49 | 0.62 | 0.61 | 0.61 |
| 8 | 0.35 | 0.36 | 0.43 | 0.45 | 0.56 | 0.59 | 0.67 | 0.69 |
| 9 | 0.22 | 0.24 | 0.21 | 0.22 | 0.51 | 0.60 | 0.48 | 0.59 |
| 10 | 0.37 | 0.47 | 0.49 | 0.42 | 1.03 | 1.45 | 1.63 | 1.43 |
| 11 | 0.19 | 0.27 | 0.26 | 0.20 | 0.41 | 0.56 | 0.54 | 0.48 |
| 12 | 0.61 | 0.68 | 0.63 | 0.60 | 0.83 | 1.04 | 1.03 | 0.97 |
| 13 | 0.07 | 0.17 | 0.31 | 0.37 | 0.46 | 0.74 | 0.96 | 0.93 |
| 14 | 0.30 | 0.30 | 0.31 | 0.33 | 0.64 | 0.65 | 0.67 | 0.71 |
| 15 | 0.32 | 0.32 | 0.43 | 0.42 | 0.62 | 0.61 | 0.79 | 0.75 |

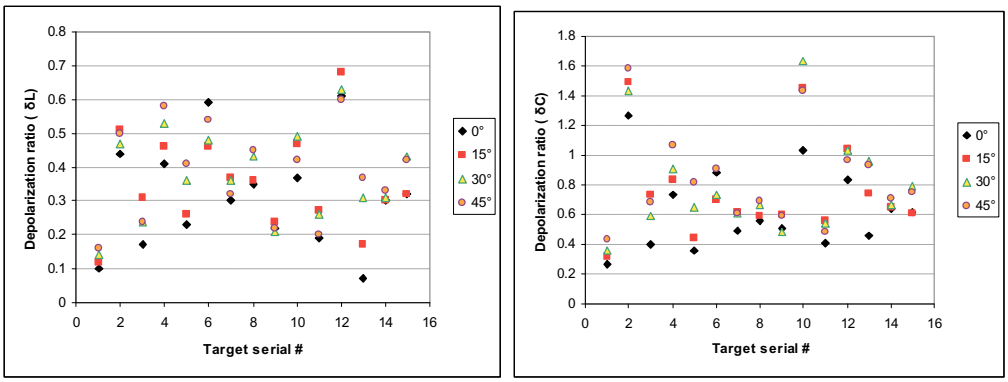


(a) $\delta_L$ (b) $\delta_C$

***Figure 6****. Depolarization ratio change with incident angle. (a) linear polariztaion (b) circular polarization*

For most insulation targets (#4 - #15), their depolarization ratios increase with incident angle. However, for targets with very rough surfaces, such as targets #7, #9 and #14, the depolarization ratio change with incident angle is not as obvious as for other targets. Depolarization ratio of target #13 at incident angle 0° is very small, but its depolarization ratio changes dramatically when incident angle increases. Targets #9 and #11 are of dark colors

and show depolarization ratios close to that from 2% Spectralon and black board. Targets with dark colors show their depolarization ratios at least 50% smaller than values of other targets. We know targets with light color usually show higher reflectivity than targets with dark color. Is the depolarization ratio of targets related to their reflectivity? If it is, what is the relationship between the depolarization ratio and reflectivity? Table 3 shows the relative reflectivity of each target on panel 1, and figure 7 is a graphical representation of the same result, i.e: the reflectivity change with incident angle.

***Table 3.*** *Reflectivity of targets on panel 1 at different incident angle*

| Target # | Relative reflectivity | | | | | | | |
|---|---|---|---|---|---|---|---|---|
| | Linear illumination | | | | Circular illumination | | | |
| | 0° | 15° | 30° | 45° | 0° | 15° | 30° | 45° |
| 1 | 0.08 | 0.07 | 0.06 | 0.06 | 0.09 | 0.08 | 0.07 | 0.07 |
| 2 | 1.00 | 1.00 | 1.00 | 1.00 | 1.00 | 1.00 | 1.00 | 1.00 |
| 3 | 0.11 | 0.10 | 0.06 | 0.07 | 0.11 | 0.09 | 0.06 | 0.08 |
| 4 | 2.17 | 1.92 | 1.51 | 1.15 | 1.68 | 1.33 | 1.15 | 1.25 |
| 5 | 1.69 | 1.29 | 1.01 | 0.75 | 1.45 | 1.02 | 0.78 | 0.92 |
| 6 | 2.56 | 2.25 | 2.00 | 1.81 | 1.94 | 1.60 | 1.31 | 1.77 |
| 7 | 0.98 | 0.81 | 0.70 | 0.76 | 0.74 | 0.54 | 0.62 | 0.77 |
| 8 | 1.03 | 1.02 | 0.76 | 0.86 | 0.81 | 0.65 | 0.63 | 0.86 |
| 9 | 0.24 | 0.25 | 0.22 | 0.24 | 0.20 | 0.19 | 0.18 | 0.28 |
| 10 | 1.09 | 2.85 | 2.07 | 1.90 | 1.84 | 2.29 | 2.19 | 2.05 |
| 11 | 0.19 | 0.19 | 0.16 | 0.24 | 0.20 | 0.14 | 0.17 | 0.22 |
| 12 | 2.09 | 1.92 | 1.35 | 1.63 | 1.10 | 1.12 | 1.18 | 1.53 |
| 13 | 0.59 | 0.41 | 0.22 | 0.26 | 1.14 | 0.43 | 0.25 | 0.30 |
| 14 | 0.66 | 0.53 | 0.44 | 0.50 | 0.59 | 0.45 | 0.44 | 0.53 |
| 15 | 0.78 | 0.81 | 0.61 | 0.64 | 0.72 | 0.59 | 0.55 | 0.62 |

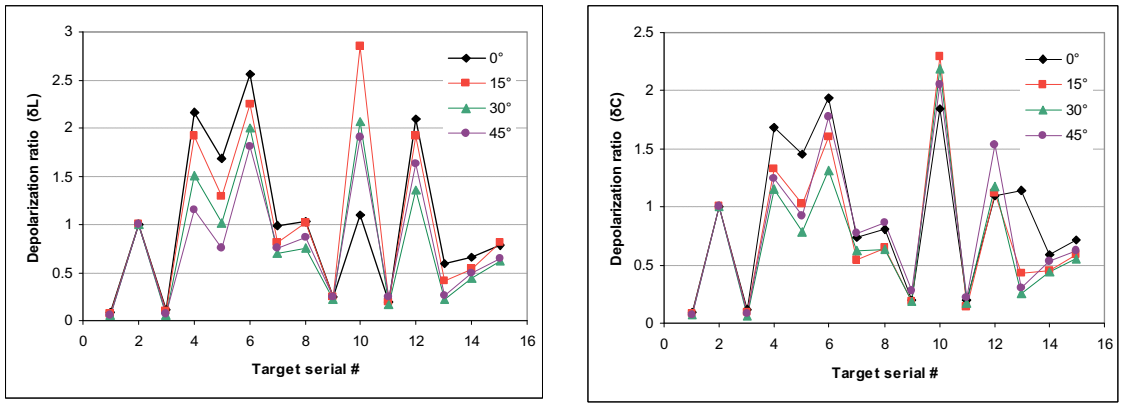


(a) Linear (b) Circular

***Figure 7.*** *Reflectivity change with incident angle. (a) linear polarization illumination (b) circular polarization illumination*

Opposite to the depolarization ratio, the reflectivity of most targets decreases with incident angle (from 0° to 30 °) with a few exceptions. The reflectivities of targets #9 and #11 are

close to each other, and are the smallest among all the insulation materials being examined. They are very close to the reference target of the 2% Spectralon. Figure 8 is a plot of depolarization ratios as a function of reflectivity.

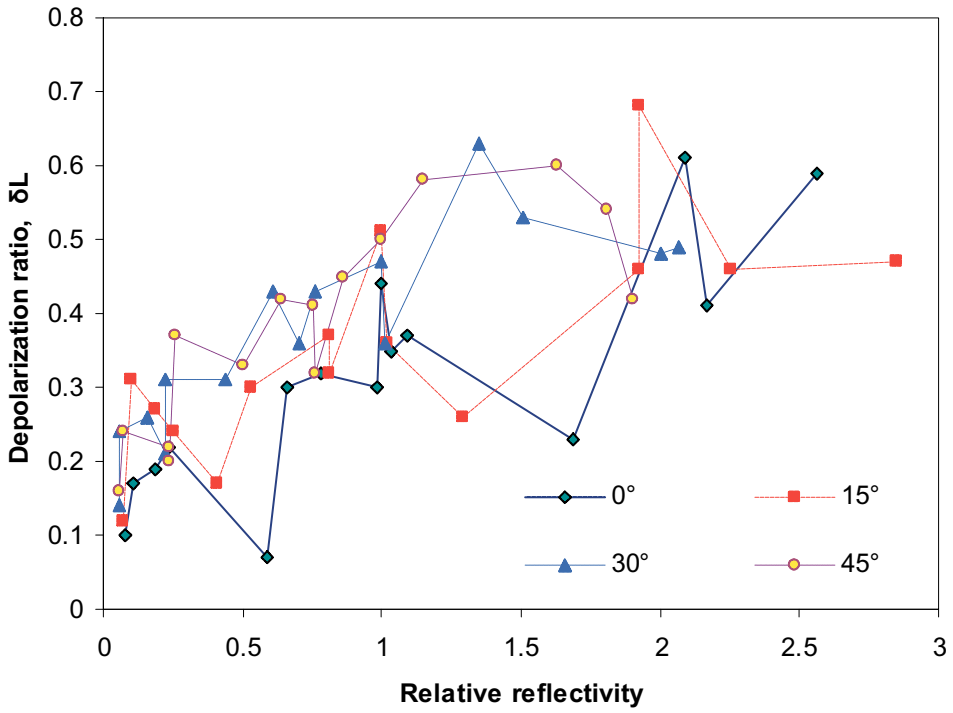


***Figure 8.*** *Insulation targets linear depolarization ratio as a function of relative reflectivity*

From Fig 8, one can see that the depolarization ratio does not strictly increase with reflectivity, but the general trend is that targets with higher reflectivity usually have high depolarization ratios too, no matter what the incident angle is.

This may be seen as an instance of what has been termed the Umov effect. This effect states that highly reflecting though rough surfaces reflect light after multiple scatterings either from the surface or from within the volume. These multiple scattering processes will cause a higher degree of depolarization. To the contrary, lowly reflecting surfaces are seen to be highly absorbing surface from which only the first mirror-like reflection has been sent back. Hence the low depolarization for that single reflection.

Other instances of this effect will be seen with the other materials studied here.

## 4.2 Panel 2 – Wood

The arrangement of targets on panel 2 is shown in Fig 9, and description of targets on the panel is listed in table 4. The corresponding analysis results of depolarization ratios and their change with incident angle are shown in Table 5 and Figure 10, respectively. It is found that these targets can be grouped in 4 categories based on their depolarization ratios. One is {4,5,9,10,11} with depolarization ratios at around 0.35. The second group is {6,8} which shows fast increase rate from 0° to 15°, then remains at a value around 0.45. The third group is {7,12,14} with depolarization ratios of about 0.25. The last one with the smallest depolarization is target 13, the black paper.

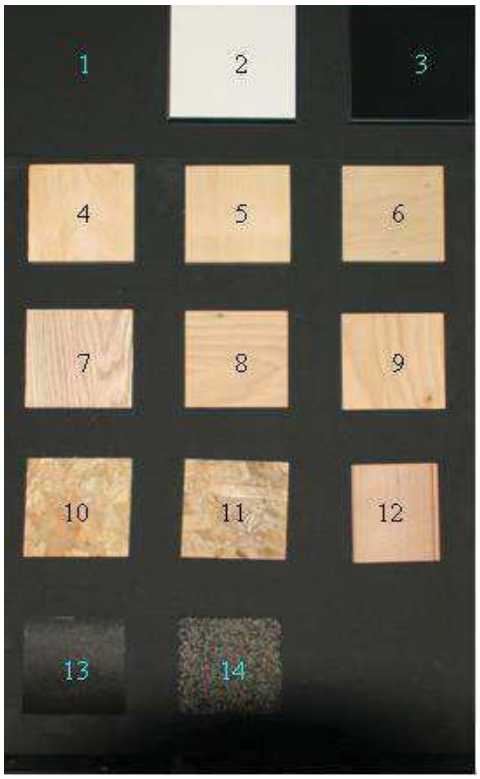


*Figure 9. Panel 2- wood*

***Table 4.*** *List of targets on panel 2*

**Panel 2- Wood**

1. Black board
2. 99% Spectralon
3. 2% Spectralon
4. Pine
5. Spruce
6. Cherry birch
7. Oak
8. Horizontal Plywood
9. Vertical Plywood
10. Oriented strand board
11. Rip board
12. Cedar
13. Black paper
14. Asphalt shingles
15. black board

***Table 5.*** *Depolarization ratio of wood targets on panel 2 at different incident angle*

| Target # | Depolarization ratio | | | | | | | |
|---|---|---|---|---|---|---|---|---|
| | $\delta_L$ | | | | $\delta_C$ | | | |
| | 0° | 15° | 30° | 45° | 0° | 15° | 30° | 45° |
| 1 | 0.09 | 0.12 | 0.14 | 0.18 | 0.24 | 0.30 | 0.36 | 0.49 |
| 2 | 0.46 | 0.50 | 0.50 | 0.47 | 1.34 | 1.47 | 1.46 | 1.52 |
| 3 | 0.19 | 0.20 | 0.22 | 0.25 | 0.42 | 0.47 | 0.55 | 0.65 |
| 4 | 0.33 | 0.35 | 0.38 | 0.37 | 1.07 | 1.13 | 1.26 | 1.24 |
| 5 | 0.32 | 0.30 | 0.32 | 0.33 | 1.09 | 1.04 | 1.17 | 1.26 |
| 6 | 0.28 | 0.42 | 0.42 | 0.45 | 1.05 | 1.42 | 1.38 | 1.53 |
| 7 | 0.22 | 0.28 | 0.30 | 0.29 | 0.99 | 1.15 | 1.18 | 1.16 |
| 8 | 0.33 | 0.42 | 0.47 | 0.41 | 1.25 | 1.47 | 1.50 | 1.44 |
| 9 | 0.36 | 0.39 | 0.35 | 0.31 | 1.35 | 1.34 | 1.33 | 1.19 |
| 10 | 0.32 | 0.31 | 0.36 | 0.34 | 1.08 | 1.07 | 1.21 | 1.24 |
| 11 | 0.35 | 0.35 | 0.38 | 0.36 | 0.97 | 0.99 | 1.14 | 1.24 |
| 12 | 0.21 | 0.24 | 0.23 | 0.25 | 0.78 | 0.93 | 0.98 | 1.08 |
| 13 | 0.07 | 0.10 | 0.15 | 0.19 | 0.18 | 0.26 | 0.41 | 0.49 |
| 14 | 0.25 | 0.25 | 0.27 | 0.25 | 0.67 | 0.70 | 0.77 | 0.75 |
| 15 | 0.07 | 0.10 | 0.12 | 0.14 | 0.18 | 0.25 | 0.29 | 0.36 |

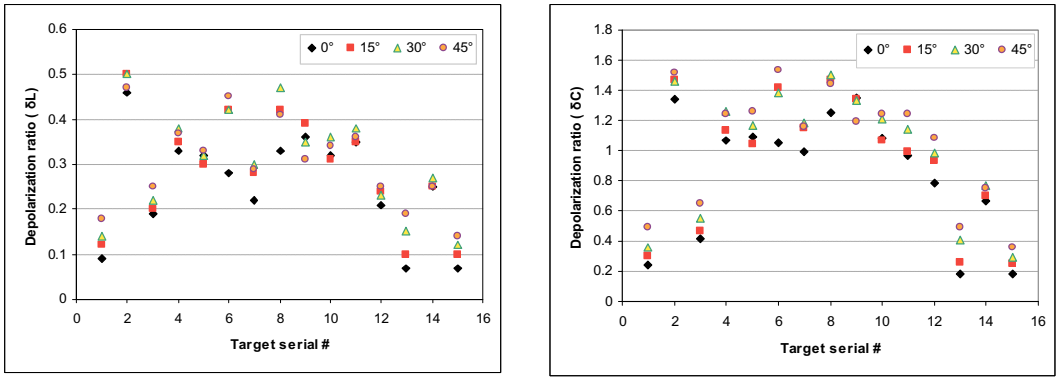


**(a) Linear** **(b) Circular**

***Figure 10****. Depolarization ratios of wood targets and their change with incident angle for linear and circular polarization illumination*

Depolarization ratios of wood targets increase with light incident angle for most targets from 0° to 45°, with a few decreasing when incident angle increased from 30° to 45°. And, from figure 10 and Table 5, we observe that the depolarization ratio of wood targets with dark color is much smaller than other targets. Is there direct relationship between the depolarization ratio and their reflectivity? We will find out by comparing the depolarization ratio and associated target reflectivity.

***Table 6. Reflectivity** of wood targets on panel 2 at different incident angle*

| Target # | Relative reflectivity | | | | | | | |
|---|---|---|---|---|---|---|---|---|
| | Linear illumination | | | | Circular illumination | | | |
| | 0° | 15° | 30° | 45° | 0° | 15° | 30° | 45° |
| 1 | 0.05 | 0.04 | 0.04 | 0.04 | 0.06 | 0.05 | 0.04 | 0.04 |
| 2 | 1.00 | 1.00 | 1.00 | 1.00 | 1.00 | 1.00 | 1.00 | 1.00 |
| 3 | 0.07 | 0.06 | 0.05 | 0.06 | 0.08 | 0.05 | 0.04 | 0.06 |
| 4 | 0.27 | 0.34 | 0.39 | 0.47 | 0.45 | 0.47 | 0.32 | 0.32 |
| 5 | 0.24 | 0.47 | 0.42 | 0.51 | 0.52 | 0.85 | 0.38 | 0.43 |
| 6 | 0.03 | 0.07 | 0.38 | 0.36 | 0.07 | 0.21 | 0.33 | 0.28 |
| 7 | 0.30 | 0.42 | 0.35 | 0.47 | 0.60 | 0.68 | 0.32 | 0.36 |
| 8 | 0.18 | 0.25 | 0.43 | 0.48 | 0.42 | 0.64 | 0.35 | 0.36 |
| 9 | 0.03 | 0.04 | 0.37 | 0.52 | 0.05 | 0.14 | 0.42 | 0.45 |
| 10 | 0.43 | 0.21 | 0.22 | 0.27 | 0.35 | 0.27 | 0.27 | 0.30 |
| 11 | 0.21 | 0.19 | 0.17 | 0.18 | 0.26 | 0.24 | 0.19 | 0.16 |
| 12 | 0.21 | 0.19 | 0.19 | 0.24 | 0.32 | 0.25 | 0.22 | 0.22 |
| 13 | 0.05 | 0.02 | 0.02 | 0.02 | 0.06 | 0.03 | 0.02 | 0.02 |
| 14 | 0.05 | 0.06 | 0.07 | 0.09 | 0.07 | 0.07 | 0.08 | 0.09 |
| 15 | 0.03 | 0.03 | 0.03 | 0.03 | 0.04 | 0.04 | 0.03 | 0.03 |

The reflectivity of wood targets for different incident angle is shown in Table 6 and Figure 11, respectively. Dark targets are seen to have smaller reflectivities and their change with incident angle is negligible when compared to other targets. Figure 12 shows the relationship for wood targets between the reflectivity and depolarization ratios. The overall trend is a small increase of depolarization ratio of wood targets with reflectivity.

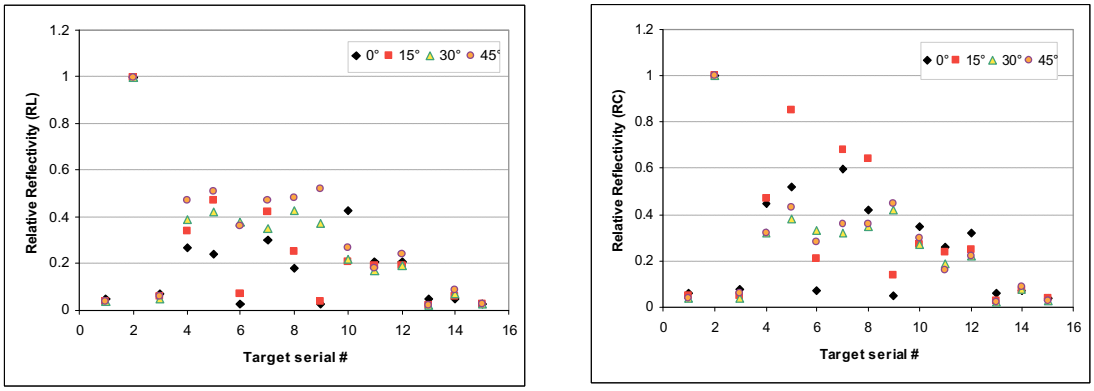


(a) Linear (b) Circular

***Figure 11**. Reflectivity change with incident angle. (a) linear polarization illumination (b) circular polarization illumination*

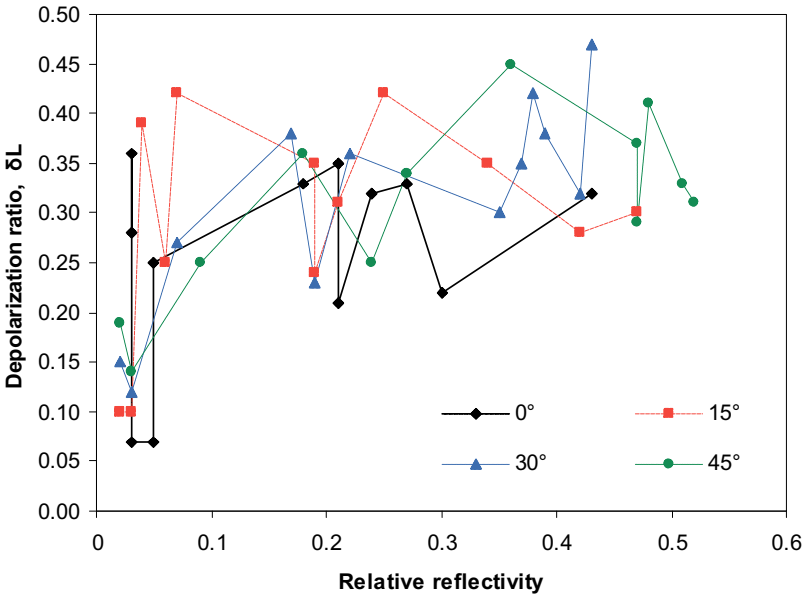


***Figure 12.*** *Wood targets linear depolarization ratio as a function of relative reflectivity.*

## 4.3 Panel 3 – Metals

Metal targets examined are shown in Fig. 13. The description of each metal target can be found in table 7. The analyzed depolarization ratios and reflectivities are shown in tables 8 and 9 respectively, and Figures 14 and 15 show the linear and circular depolarization ratios and reflectivity respectively, and their change with incident angle.

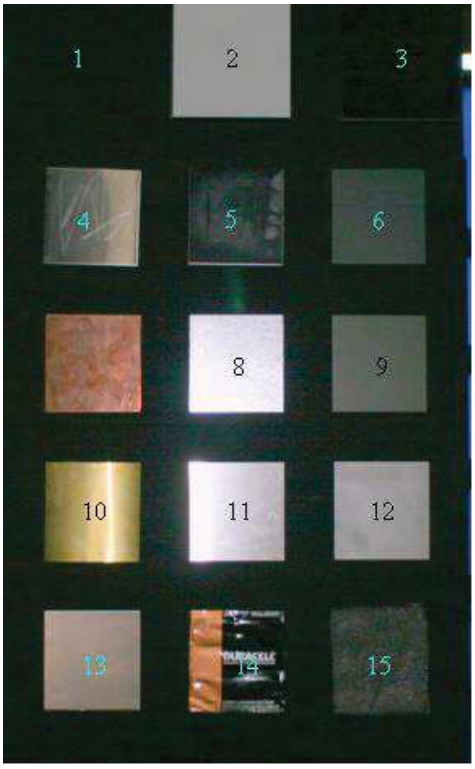


*Figure 13. Picture of targets on panel 3*

***Table 7.*** *Targets on panel 3*

| **Panel 3- Metal** |
|---|
| 1. Black board |
| 2. 99% Spectralon |
| 3. 2% Spectralon |
| 4. Vertical Stainless Steel |
| 5. Horizontal Stainless Steel |
| 6. Green forest Steel |
| 7. Copper |
| 8. Galvanized Steel |
| 9. Light Green Steel |
| 10. Brass |
| 11. Aluminum |
| 12. Sand-blasted Steel |
| 13. Natural Steel |
| 14. 6-volts Batteries (DuracellØ ) |
| 15. Steel Wool |

Just like above discussed insulation and wood targets, depolarization ratios of metal targets increase with incident angle, here without any exception. However, metals depolarization ratios are close to each other except targets #6 and #9 whose depolarization ratios are at least double of other metal targets' ratios.

Some metal targets showed a lot more reflectivity such as target #8, #10, and #11, but only at incident angle 0°. When incident angle was increased to 15°, their reflectivity decreased dramatically, then decreased little when incident angle further increased, as shown in figure 15.

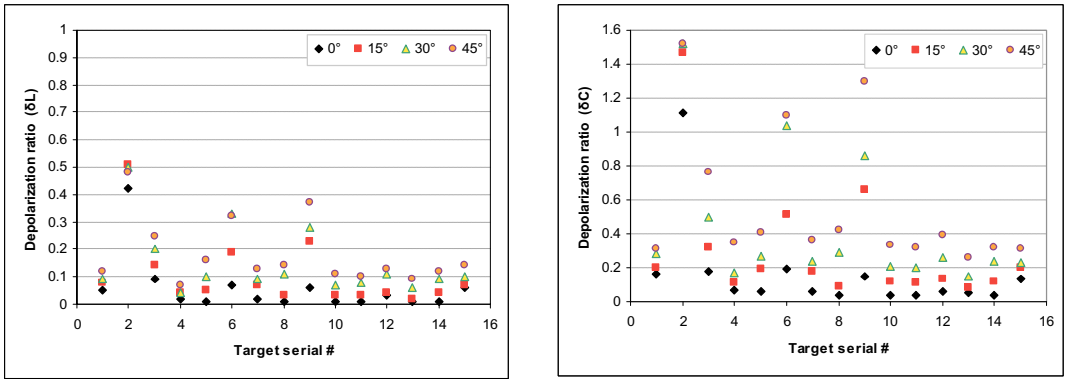


(a) Linear (b) Circular

***Figure 14.*** *Depolarization ratios of metals and their change with incident angle*

***Table 8.*** *Depolarization ratio of metal targets on panel 3 at different incident angle*

| Target # | Depolarization ratio | | | | | | | |
|---|---|---|---|---|---|---|---|---|
| | $\delta_L$ | | | | $\delta_C$ | | | |
| | 0° | 15° | 30° | 45° | 0° | 15° | 30° | 45° |
| 1 | 0.05 | 0.08 | 0.09 | 0.12 | 0.16 | 0.20 | 0.28 | 0.31 |
| 2 | 0.42 | 0.51 | 0.50 | 0.48 | 1.11 | 1.47 | 1.52 | 1.52 |
| 3 | 0.09 | 0.14 | 0.20 | 0.25 | 0.18 | 0.32 | 0.50 | 0.76 |
| 4 | 0.02 | 0.04 | 0.04 | 0.07 | 0.07 | 0.11 | 0.17 | 0.35 |
| 5 | 0.01 | 0.05 | 0.10 | 0.16 | 0.06 | 0.19 | 0.27 | 0.41 |
| 6 | 0.07 | 0.19 | 0.33 | 0.32 | 0.19 | 0.51 | 1.04 | 1.10 |
| 7 | 0.02 | 0.07 | 0.09 | 0.13 | 0.06 | 0.18 | 0.24 | 0.36 |
| 8 | 0.01 | 0.03 | 0.11 | 0.14 | 0.04 | 0.09 | 0.29 | 0.42 |
| 9 | 0.06 | 0.23 | 0.28 | 0.37 | 0.15 | 0.66 | 0.86 | 1.30 |
| 10 | 0.01 | 0.03 | 0.07 | 0.11 | 0.04 | 0.12 | 0.21 | 0.33 |
| 11 | 0.01 | 0.03 | 0.08 | 0.10 | 0.04 | 0.11 | 0.20 | 0.32 |
| 12 | 0.03 | 0.04 | 0.11 | 0.13 | 0.06 | 0.13 | 0.26 | 0.39 |
| 13 | 0.01 | 0.02 | 0.06 | 0.09 | 0.05 | 0.08 | 0.15 | 0.26 |
| 14 | 0.01 | 0.04 | 0.09 | 0.12 | 0.04 | 0.12 | 0.24 | 0.32 |
| 15 | 0.06 | 0.07 | 0.10 | 0.14 | 0.13 | 0.20 | 0.23 | 0.31 |

***Table 9.*** *Relative reflectivity of metal targets on panel 3 at different incident angle*

| Target # | Relative reflectivity | | | | | | | |
|---|---|---|---|---|---|---|---|---|
| | Linear illumination | | | | Circular illumination | | | |
| | 0° | 15° | 30° | 45° | 0° | 15° | 30° | 45° |
| 1 | 0.07 | 0.07 | 0.09 | 0.07 | 0.11 | 0.10 | 0.09 | 0.07 |
| 2 | 1.00 | 1.00 | 1.00 | 1.00 | 1.00 | 1.00 | 1.00 | 1.00 |
| 3 | 0.08 | 0.05 | 0.10 | 0.07 | 0.11 | 0.06 | 0.10 | 0.07 |
| 4 | 0.29 | 0.26 | 0.25 | 0.17 | 0.54 | 0.30 | 0.27 | 0.18 |
| 5 | 0.99 | 0.14 | 0.11 | 0.08 | 1.77 | 0.17 | 0.10 | 0.07 |
| 6 | 0.42 | 0.32 | 0.25 | 0.19 | 0.69 | 0.33 | 0.22 | 0.17 |
| 7 | 1.24 | 0.43 | 0.39 | 0.33 | 2.15 | 0.46 | 0.36 | 0.27 |
| 8 | 8.29 | 0.97 | 0.36 | 0.27 | 14.08 | 1.12 | 0.37 | 0.23 |
| 9 | 0.92 | 0.73 | 0.70 | 0.91 | 1.51 | 0.79 | 0.67 | 0.66 |
| 10 | 4.56 | 0.35 | 0.15 | 0.09 | 7.24 | 0.41 | 0.16 | 0.08 |
| 11 | 3.02 | 0.19 | 0.10 | 0.08 | 5.27 | 0.22 | 0.11 | 0.08 |
| 12 | 1.82 | 1.18 | 0.36 | 0.27 | 2.46 | 0.72 | 0.39 | 0.23 |
| 13 | 0.86 | 0.17 | 0.08 | 0.04 | 1.30 | 0.18 | 0.08 | 0.05 |
| 14 | 0.77 | 0.12 | 0.06 | 0.05 | 1.17 | 0.13 | 0.07 | 0.05 |
| 15 | 0.23 | 0.17 | 0.20 | 0.17 | 0.37 | 0.21 | 0.23 | 0.17 |

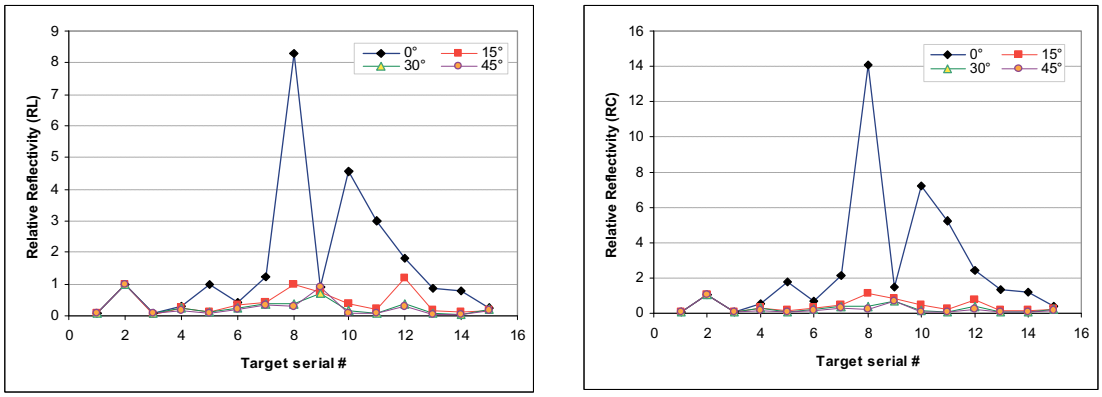


(a) Linear (b) Circular

***Figure 15****. Reflectivity change of metal targets with incident angle.*

When we look at the depolarization ratios from figure 14 and reflectivities from figure 15, it is found that targets with high reflectivities do show lower depolarization ratios; in fact for metal, high reflectivity goes with low depolarization ratio for illumination angle close to 0°. No Umov effect can be seen on metals since their surface usually is smooth, thus not prone to generating multiple scattering processes. If we ignore a few outliers with relatively higher depolarization ratios, we can find from figure 14 that most metal targets showed depolarization ratios close to each other.

## 4.4 Panel 4 – Environmental targets

Panel 4 consists of environmental targets such as plastic and beer bottles and different cans, as listed in table 10. Figure 16 shows targets without beer bottles which were measured separately. Figures 17 shows depolarization ratio and reflectivity change with incident angle. The analysed results of environmental targets are listed in Table 11 and 12.

Since it was difficult to locate the position of the brown beer bottle based on Andor image, this target was not included here. Figure 18 shows that reflectivities of environmental targets dropped when incident angle changed from 0° to 15°, then increased when incident angle further increased. Some initial reflectivity drops are dramatic such as for target 5. From 15° to 45°, the reflectivity increased approximately linearly with incident angle for most environmental targets.

Target #6 showed smallest reflectivity because of its dark color. Crushed cans and plastic bottles showed reflectivities comparable to those obtained from undamaged cans and bottles. White cotton showed much higher reflectivity than other targets on the same panel, and at 45° incident angle, the target showed a reflectivity comparable to that of white Spectralon.


*Figure 16. Picture of targets on panel 4*

***Table 10.*** *List of targets on panel 4*

| Panel- Environment |
|---|
| 1. Black board |
| 2. 99% Spectralon |
| 3. 2% Spectralon |
| 4. Crushed Soda Can |
| 5. Soda Can |
| 6. Polyester |
| 7. Jute |
| 8. Cotton |
| 9. Chiffon |
| 10. Transparent Plastic Bottle |
| 11. Crushed Transparent Plastic Bottle |
| 12. Coloured Plastic Bottle |
| 13. Beer bottle brown, not shown |
| 14. Beer bottle clear, not shown |

***Table 11.*** *Depolarization ratio of environmental targets on panel4 at different incident angle*

| Target # | Depolarization ratio | | | | | | | |
|---|---|---|---|---|---|---|---|---|
| | $\delta_L$ | | | | $\delta_C$ | | | |
| | 0° | 15° | 30° | 45° | 0° | 15° | 30° | 45° |
| 1 | 0.08 | 0.14 | 0.14 | 0.21 | 0.22 | 0.34 | 0.34 | 0.47 |
| 2 | 0.56 | 0.62 | 0.55 | 0.52 | 1.57 | 1.80 | 1.65 | 1.65 |
| 3 | 0.16 | 0.19 | 0.18 | 0.47 | 0.36 | 0.45 | 0.49 | 1.41 |
| 4 | 0.14 | 0.22 | 0.19 | 0.16 | 0.33 | 0.57 | 0.56 | 0.45 |
| 5 | 0.05 | 0.26 | 0.21 | 0.21 | 0.14 | 0.82 | 0.55 | 0.54 |
| 6 | 0.15 | 0.16 | 0.17 | 0.17 | 0.37 | 0.45 | 0.45 | 0.46 |
| 7 | 0.40 | 0.42 | 0.40 | 0.56 | 0.94 | 1.08 | 0.99 | 1.24 |
| 8 | 0.62 | 0.57 | 0.58 | 0.56 | 1.29 | 1.25 | 1.30 | 1.26 |
| 9 | 0.46 | 0.39 | 0.40 | 0.44 | 1.03 | 0.91 | 1.02 | 1.23 |
| 10 | 0.37 | 0.64 | 0.44 | 0.39 | 0.51 | 1.12 | 0.94 | 0.85 |
| 11 | 0.37 | 0.43 | 0.43 | 0.70 | 0.84 | 1.06 | 1.06 | 1.19 |
| 12 | 0.37 | 0.41 | 0.40 | 0.54 | 1.23 | 1.46 | 1.36 | 1.80 |
| 13 | - | - | - | - | - | - | - | - |
| 14 | 0.17 | 0.26 | 0.12 | 0.28 | 0.44 | 0.73 | 0.30 | 0.79 |

***Table 12.*** *Relative reflectivity of environmental targets on panel4 at different incident angle*

| Target # | Relative reflectivity | | | | | | | |
|---|---|---|---|---|---|---|---|---|
| | Linear illumination | | | | Circular illumination | | | |
| | 0° | 15° | 30° | 45° | 0° | 15° | 30° | 45° |
| 1 | 0.07 | 0.05 | 0.05 | 0.04 | 0.06 | 0.06 | 0.05 | 0.05 |
| 2 | 1.00 | 1.00 | 1.00 | 1.00 | 1.00 | 1.00 | 1.00 | 1.00 |
| 3 | 0.07 | 0.07 | 0.09 | 0.14 | 0.06 | 0.06 | 0.10 | 0.08 |
| 4 | 0.20 | 0.11 | 0.10 | 0.21 | 0.16 | 0.11 | 0.11 | 0.23 |
| 5 | 0.48 | 0.11 | 0.16 | 0.21 | 0.44 | 0.12 | 0.16 | 0.22 |
| 6 | 0.03 | 0.02 | 0.05 | 0.05 | 0.03 | 0.03 | 0.05 | 0.05 |
| 7 | 0.23 | 0.16 | 0.31 | 0.28 | 0.16 | 0.13 | 0.21 | 0.34 |
| 8 | 0.55 | 0.49 | 0.60 | 1.13 | 0.53 | 0.42 | 0.61 | 0.90 |
| 9 | 0.31 | 0.24 | 0.36 | 0.49 | 0.30 | 0.24 | 0.35 | 0.60 |
| 10 | 0.28 | 0.08 | 0.23 | 0.62 | 0.21 | 0.07 | 0.19 | 0.35 |
| 11 | 0.30 | 0.12 | 0.24 | 0.33 | 0.25 | 0.12 | 0.29 | 0.25 |
| 12 | 0.19 | 0.12 | 0.24 | 0.42 | 0.17 | 0.10 | 0.30 | 0.45 |
| 13 | - | - | - | - | - | - | - | - |
| 14 | 0.20 | 0.20 | 0.44 | 0.42 | 0.21 | 0.16 | 0.49 | 0.42 |

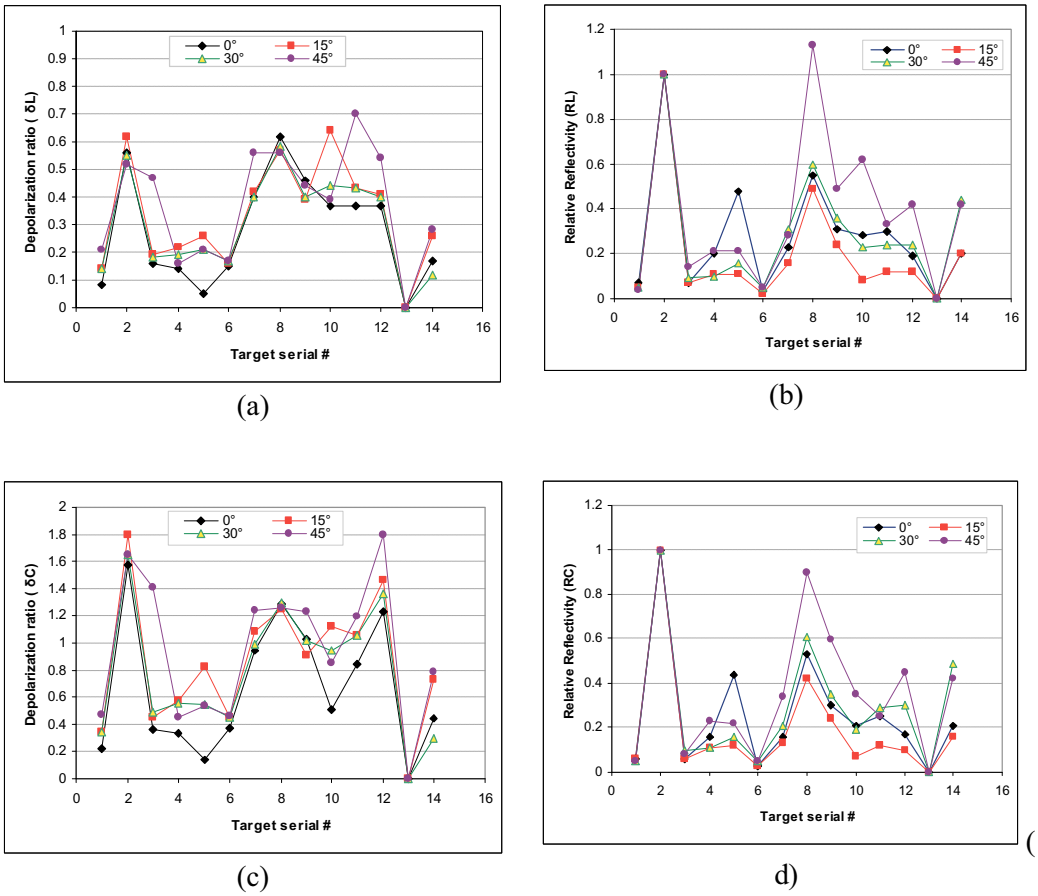


***Figure 17.*** *Depolarization ratio (left) and reflectivity (right) of environmental targets change with incident angle. (a) and (b) are for linear polarization, (c) and (d) are circular polarization.*

From figure 17, we see that generally, large reflectivity usually associates with large depolarization ratio. There is no clear relationship, however, for environmental targets, between depolarization ratio and reflectivity as shown on Figure 18.

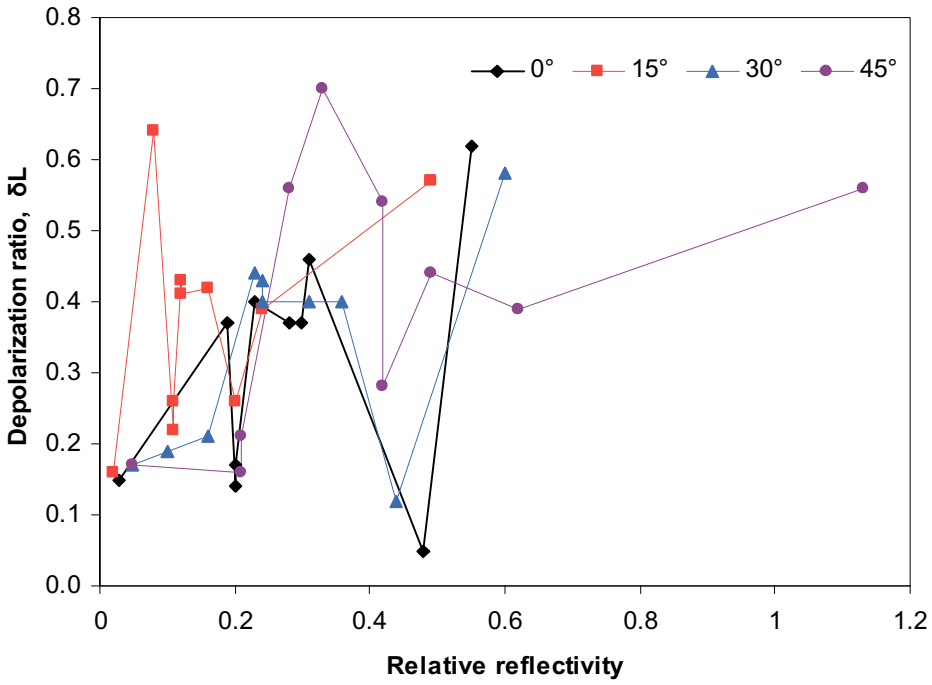


***Figure 18**. Environmental targets linear depolarization ratio as a function of relative reflectivity.*

## 4.5 Panel 5 – Sand papers

Sand papers with different colors and grit numbers are listed in Table 13, and their image is shown in figure 19. The analysis results of depolarization ratio and reflectivity are shown in table 14 and 15, respectively.

Generally, all targets have their depolarization ratios increase linearly with incident angle, with some exceptions for circular polarization from 30 ° to 45°. Circular depolarization ratios are usually 2.5 ~ 3 times larger than linear ones, with exception of target 13 which showed much higher ratio. For the reflectivity, it is found that all targets reflectivities decrease with incident angle from 0° to 30°, and then slightly increase or remain unchanged from incident angle 30° to 45°.


*Figure 19. Picture of targets on panel 5*

***Table 13.*** *List of targets on panel 5*

| **Panel 5- Sandpaper** |
|---|
| 1. Black board |
| 2. 99% Spectralon |
| 3. 2% Spectralon |
| 4. Sand paper 50 |
| 5. Sand paper 100 |
| 6. Sand paper 220 |
| 7. Sand paper 400 |
| 8. Sand paper 600 |
| 9. Sand paper 1000 |
| 10. Sand paper 1500 |
| 11. Paper bag |
| 12. Carton |
| 13. Transparent Plastic Bag |
| 14. White Plastic bag |

***Table 14.*** *Depolarization ratio of sand papers on panel 5 at different incident angle*

| **Target #** | **Depolarization ratio** | | | | | | | |
|---|---|---|---|---|---|---|---|---|
| | **ΔL** | | | | **ΔC** | | | |
| | **0°** | **15°** | **30°** | **45°** | **0°** | **15°** | **30°** | **45°** |
| 1 | 0.07 | 0.10 | 0.14 | 0.16 | 0.26 | 0.32 | 0.36 | 0.42 |
| 2 | 0.45 | 0.51 | 0.52 | 0.60 | 1.32 | 1.52 | 1.56 | 1.42 |
| 3 | 0.13 | 0.24 | 0.28 | 0.28 | 0.57 | 0.67 | 0.72 | 0.57 |
| 4 | 0.36 | 0.41 | 0.46 | 0.46 | 0.98 | 1.14 | 1.40 | 1.21 |
| 5 | 0.46 | 0.48 | 0.48 | 0.49 | 1.32 | 1.48 | 1.50 | 1.32 |
| 6 | 0.49 | 0.46 | 0.53 | 0.50 | 1.24 | 1.24 | 1.48 | 1.30 |
| 7 | 0.13 | 0.14 | 0.15 | 0.19 | 0.32 | 0.35 | 0.40 | 0.57 |
| 8 | 0.27 | 0.32 | 0.35 | 0.39 | 0.74 | 0.90 | 1.05 | 0.75 |
| 9 | 0.16 | 0.18 | 0.24 | 0.28 | 0.39 | 0.46 | 0.66 | 0.74 |
| 10 | 0.22 | 0.25 | 0.29 | 0.30 | 0.67 | 0.73 | 0.85 | 0.80 |
| 11 | 0.31 | 0.39 | 0.41 | 0.43 | 1.03 | 1.25 | 1.42 | 1.29 |
| 12 | 0.30 | 0.34 | 0.40 | 0.39 | 0.90 | 1.08 | 1.35 | 1.35 |
| 13 | 0.07 | 0.20 | 0.35 | 0.46 | 0.96 | 1.39 | 1.14 | 0.93 |
| 14 | 0.43 | 0.57 | 0.57 | 0.60 | 0.91 | 1.25 | 1.25 | 1.43 |

***Table 15.*** *Relative reflectivity of sand papers on panel5 at different incident angle*

| Target # | Relative reflectivity | | | | | | | |
|---|---|---|---|---|---|---|---|---|
| | Linear illumination | | | | Circular illumination | | | |
| | 0° | 15° | 30° | 45° | 0° | 15° | 30° | 45° |
| 1 | 0.10 | 0.07 | 0.06 | 0.06 | 0.11 | 0.09 | 0.06 | 0.07 |
| 2 | 1.00 | 1.00 | 1.00 | 1.00 | 1.00 | 1.00 | 1.00 | 1.00 |
| 3 | 0.14 | 0.10 | 0.08 | 0.08 | 0.12 | 0.10 | 0.08 | 0.08 |
| 4 | 0.73 | 0.56 | 0.42 | 0.46 | 0.75 | 0.62 | 0.44 | 0.46 |
| 5 | 0.73 | 0.71 | 0.52 | 0.61 | 0.79 | 0.82 | 0.52 | 0.59 |
| 6 | 1.00 | 0.99 | 0.61 | 0.66 | 1.01 | 0.91 | 0.61 | 0.61 |
| 7 | 0.16 | 0.13 | 0.08 | 0.09 | 0.22 | 0.18 | 0.08 | 0.10 |
| 8 | 0.60 | 0.50 | 0.31 | 0.30 | 0.64 | 0.56 | 0.29 | 0.28 |
| 9 | 0.27 | 0.19 | 0.11 | 0.12 | 0.28 | 0.23 | 0.11 | 0.11 |
| 10 | 0.09 | 0.06 | 0.07 | 0.09 | 0.09 | 0.07 | 0.09 | 0.11 |
| 11 | 0.26 | 0.22 | 0.21 | 0.18 | 0.32 | 0.24 | 0.22 | 0.19 |
| 12 | 0.28 | 0.24 | 0.20 | 0.23 | 0.26 | 0.24 | 0.20 | 0.24 |
| 13 | 1.04 | 0.13 | 0.10 | 0.12 | 1.35 | 0.16 | 0.11 | 0.11 |
| 14 | 0.42 | 0.34 | 0.38 | 0.42 | 0.43 | 0.32 | 0.33 | 0.40 |

Target #14 shows the largest linear depolarization among all targets on panel 5, and the target #7 the smallest one, close to the value of the 2% spectralon. Target #13 is special: its linear depolarization started from the smallest at incident angle 0°, and quickly jumped to the group of light color sand papers. The circular depolarization ratio of target 13 only increased from incident angle 0° to 15°, then decreased when incident angle further increased. Target 13 is transparent, so at normal incidence the holding board has a definite effect.

Figure 20 is a plot of the results shown in tables 14 and 15. It seems the larger the grit number, the lower the reflectivity. However, it seems, the reflectivity and depolarization have to do with the target color, the lighter the color, the higher the reflectivity, and the higher the depolarization ratio. If one compares the reflectivity and depolarization ratio, it will be noticed that normally higher reflectivity associates with higher depolarization ratio, just like other panels we have discussed above. In figure 21, we plot depolarization with respect to their reflectivity, and it confirms our previous findings. For sand papers mounted on panel #5, a linear relationship between depolarization ratio and reflectivity can be drawn. This relationship is in accord with the Umov effect.

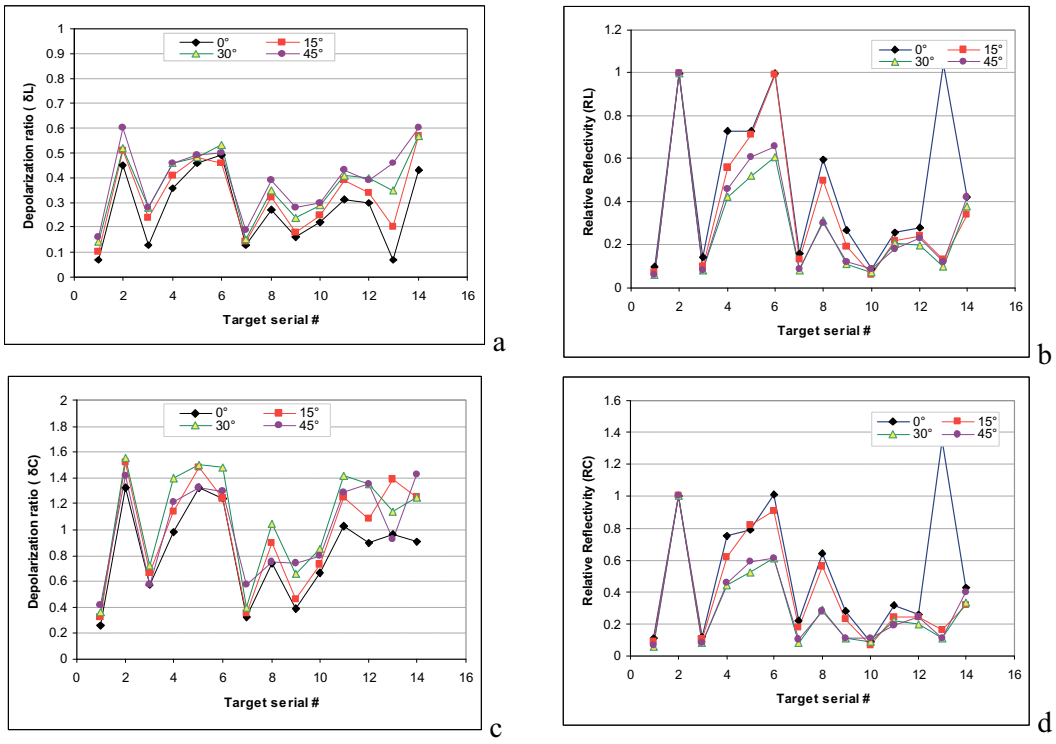


***Figure 20**. Depolarization ratio (left) and reflectivity (right) change of sand papers with incident angle. (a) and (b) are for linear polarization, (c) and (d) are circular polarization.*

.

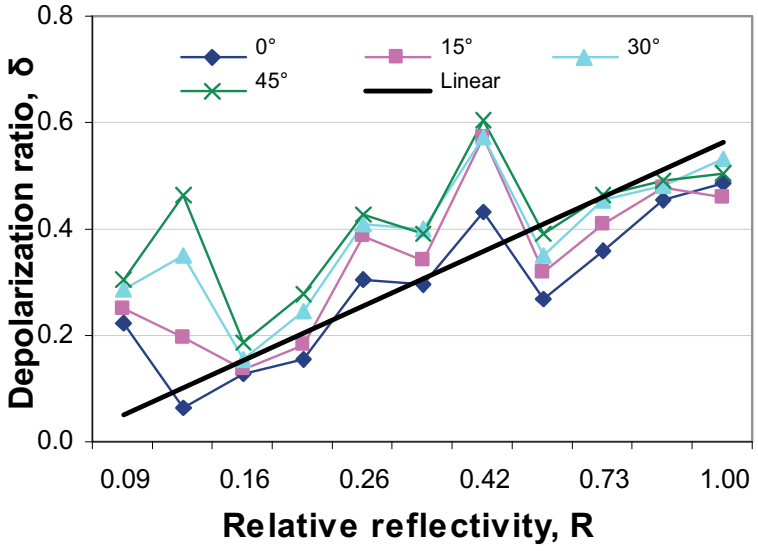


***Figure 21.** Sand paper targets linear depolarization ratio as a function of relative reflectivity.*

.

## 4.6 Panel 6 – Composite materials

Targets on panel 6 are shown in Figure 22 with material description in Table 16. Results of depolarization ratio and reflectivity of each target are shown in Tables 17 and 18, respectively. Figure 23 shows the depolarization ratio and reflectivity change with incident angle. Like most other panel targets, depolarization ratios of most subtargets increase while the reflectivity decreases with incident angle with a few exceptions.


*Figure 22. Picture of targets on panel 6*

***Table 16.*** *List of targets on panel 6*

| Panel 6- Conposite |
|---|
| 1. Black board |
| 2. 99% Spectralon |
| 3. 2% Spectralon |
| 4. Black Rubber |
| 5. Orange Silicone |
| 6. Polytetrafluoroethylene (TeflonØ ) |
| 7. Flame Retardant Sheet (Kydex Acrilic PVC) |
| 8. High Density PolyEthylene |
| 9. Nema Phenolic (Glass fiber reinforced) |
| 10. Acetal (DelrinØ ) |
| 11. Opaque Styrene |
| 12. Sand-Coloured Vinyl |
| 13. Plastic Glass |
| 14. Polycarbonate resin thermoplastic (LexanØ ) |
| 15. Tarpaulin |

***Table 17.*** *Depolarization ratio of targets on panel 6 at different incident angle*

| | $\delta_L$ | | | | $\delta_C$ | | | |
|---|---|---|---|---|---|---|---|---|
| Target | 0° | 15° | 30° | 45° | 0° | 15° | 30° | 45° |
| 1 | 0.10 | 0.11 | 0.13 | 0.16 | 0.28 | 0.32 | 0.39 | 0.45 |
| 2 | 0.46 | 0.48 | 0.50 | 0.47 | 1.27 | 1.45 | 1.53 | 1.52 |
| 3 | 0.24 | 0.29 | 0.36 | 0.35 | 0.46 | 0.64 | 0.86 | 0.77 |
| 4 | 0.05 | 0.14 | 0.21 | 0.25 | 0.09 | 0.33 | 0.55 | 0.64 |
| 5 | 0.08 | 0.22 | 0.31 | 0.32 | 0.16 | 0.53 | 0.76 | 0.89 |
| 6 | 0.52 | 0.71 | 0.74 | 0.81 | 0.70 | 1.00 | 1.08 | 1.26 |
| 7 | 0.18 | 0.24 | 0.36 | 0.37 | 0.45 | 0.73 | 1.05 | 1.31 |
| 8 | 0.53 | 0.83 | 0.74 | 0.77 | 0.66 | 1.00 | 0.86 | 1.02 |
| 9 | 0.03 | 0.34 | 0.41 | 0.41 | 0.06 | 0.92 | 1.27 | 1.25 |
| 10 | 0.42 | 0.75 | 0.83 | 0.84 | 0.49 | 0.88 | 1.00 | 1.10 |
| 11 | 0.26 | 0.55 | 0.51 | 0.53 | 0.60 | 1.57 | 1.53 | 1.81 |
| 12 | 0.28 | 0.42 | 0.44 | 0.43 | 0.90 | 1.49 | 1.63 | 1.65 |
| 13 | 0.06 | 0.13 | 0.20 | 0.28 | 0.10 | 0.30 | 0.46 | 0.73 |
| 14 | 0.80 | 0.98 | 0.80 | 0.67 | 1.30 | 1.84 | 1.66 | 1.54 |
| 15 | 0.14 | 0.20 | 0.35 | 0.43 | 0.75 | 0.91 | 1.05 | 1.16 |

***Table 18.*** *Reflectivity of targets on panel6 at different incident angle*

| Target # | Relative reflectivity | | | | | | | |
|---|---|---|---|---|---|---|---|---|
| | Linear illumination | | | | Circular illumination | | | |
| | 0° | 15° | 30° | 45° | 0° | 15° | 30° | 45° |
| 1 | 0.06 | 0.07 | 0.05 | 0.05 | 0.07 | 0.08 | 0.05 | 0.05 |
| 2 | 1.00 | 1.00 | 1.00 | 1.00 | 1.00 | 1.00 | 1.00 | 1.00 |
| 3 | 0.08 | 0.08 | 0.09 | 0.08 | 0.08 | 0.08 | 0.07 | 0.06 |
| 4 | 0.20 | 0.07 | 0.05 | 0.05 | 0.23 | 0.07 | 0.04 | 0.05 |
| 5 | 0.28 | 0.12 | 0.09 | 0.10 | 0.31 | 0.12 | 0.07 | 0.09 |
| 6 | 1.38 | 1.07 | 1.02 | 1.05 | 1.17 | 0.87 | 0.73 | 0.87 |
| 7 | 0.31 | 0.33 | 0.27 | 0.29 | 0.31 | 0.31 | 0.20 | 0.22 |
| 8 | 0.72 | 0.71 | 0.70 | 0.69 | 0.60 | 0.56 | 0.42 | 0.58 |
| 9 | 1.93 | 0.14 | 0.12 | 0.12 | 2.15 | 0.13 | 0.08 | 0.10 |
| 10 | 0.46 | 0.84 | 0.74 | 0.68 | 0.39 | 0.68 | 0.49 | 0.50 |
| 11 | 0.93 | 0.96 | 1.34 | 1.05 | 0.90 | 1.02 | 1.11 | 1.26 |
| 12 | 0.57 | 0.86 | 1.03 | 0.84 | 0.49 | 0.82 | 0.77 | 0.63 |
| 13 | 0.19 | 0.12 | 0.08 | 0.08 | 0.21 | 0.12 | 0.06 | 0.08 |
| 14 | 0.18 | 0.12 | 0.11 | 0.10 | 0.16 | 0.12 | 0.09 | 0.09 |
| 15 | 0.73 | 0.52 | 0.36 | 0.29 | 0.85 | 0.62 | 0.33 | 0.33 |

Among all the composite targets, target #9 has significantly different signature. The measurement shows that this target has very low depolarization ratio but very high reflectivity at incident angle 0°. When incident angle increased to 15 °, the reflectivity decreased dramatically. It is suspected that this target acts like a mirror. As to the relationship between depolarization ratio and reflectivity, it follows the same trend as other types of targets that generally higher reflectivity associates with higher depolarization ratio, but with a few exceptions, as shown in Figure 24.

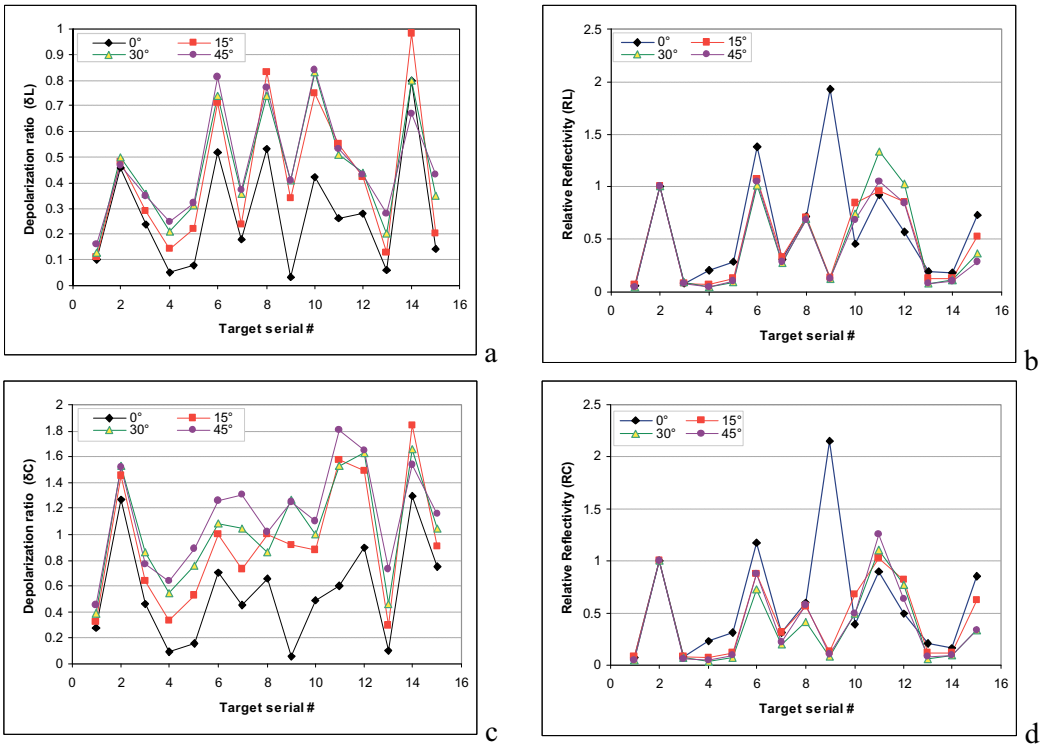


***Figure 23.*** *Depolarization ratio (left) and reflectivity (right) change of composite with incident angle. (a) and (b) are for linear polarization, (c) and (d) are circular polarization. (a) and (b) are for linear polarization, (c) and (d) are circular polarization.*

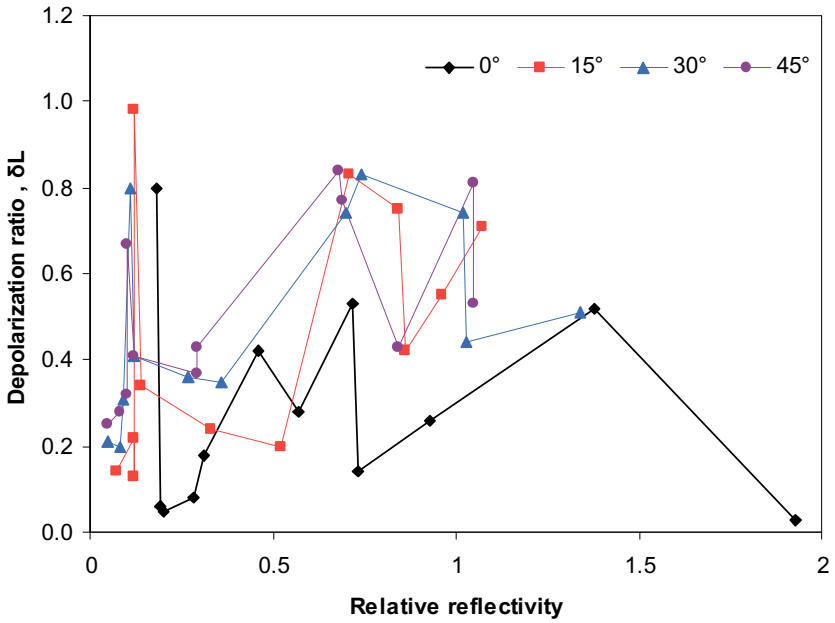


***Figure 24.*** *Composite targets linear depolarization ratio as a function of relative reflectivity.*

## 4.7 Panel 7 – Sands and other construction materials

Sands (dry and wet) and other construction materials examined are listed in table 19. The depolarization and reflectivity results are shown in figure 25. Again, depolarization ratio increases and reflectivity decreases with inciden angle for most targets. Fine sands, no matter dry or wet, always show higher depolarization ratios than coarse sands. And again, targets with higher reflectivity usually show higher depolarization too, as shown in figure 26.

***Table 19.*** *Targets description of construction material*

| Target # | Sands | Target # | Construction and grass |
|---|---|---|---|
| 1 | 99% Spectralon | 6 | - |
| 2 | Coarse sand (dry) | 7 | concrete |
| 3 | Fine sand (dry) | 8 | Asphalt |
| 4 | Coarse sand (wet) | 9 | Grass 1 |
| 5 | Fine sand (wet) | 10 | Grass 2 |

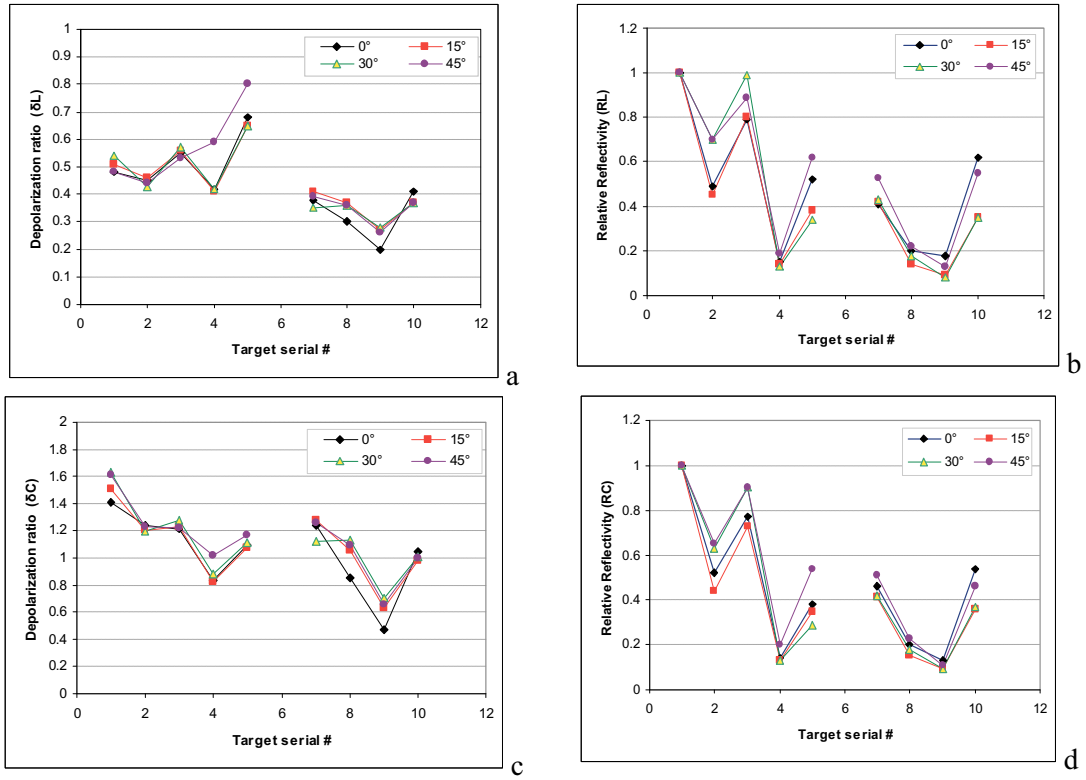


***Figure 25.*** *Depolarization ratio (left) and reflectivity (right) change of construction materials with incident angle. (a) and (b) are for linear polarization, (c) and (d) are circular polarization.*

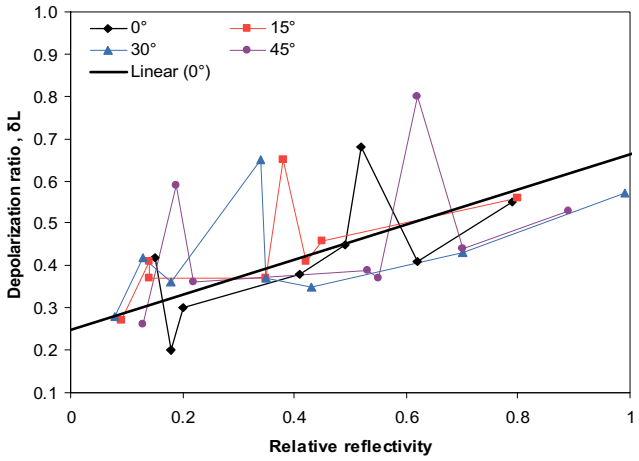


***Figure 26***. *Construction materials: linear depolarization ratio change with associated reflectivity.*

## 4.8 Summary

Based on analysis of all panel targets, targets with light color and smooth surface showed higher reflectivity than targets with dark color and rough surface. Target reflectivity from circular polarized light is usually very close to the reflectivity from linear polarized light with very few exceptions. Excep metal targets, it is also found that, for most solid targets of a given material category, targets with higher reflectivity usually show higher depolarization than targets with lower reflectivity. Depolarization ratio increases with polarized light incident angle, and circular depolarization ratio is usually 2~3 times the linear one for most targets, with a few exceptions.

Metal targets are very different from other targets. Their very high reflectivity at incident angle 0° dramatically decreases when incident angle increases from 0° to 15°, then remains little changed when incident angle further increases. However, high reflectivity metals associate with very low depolarization. For targets with rough surfaces, the influence of incident angle over depolarization and reflectivity is less important than for smooth surface targets; this is understandable because no matter what the incident angle is, to those targets with rough surfaces, the local incident angle at different spots may be different, so the total effect does not show much change.

# 5. Depolarization ratio at wavelength of 1570 nm

The above results were based on field measurements using a dual polarization imaging lidar operating at a wavelength of 532 nm. We also conducted field measurements of depolarization of solid targets using 1.57 μm wavelength Dual-Polarization Lidar, (see Ref. [3]) in September 2008. This time, targets on each panel were examined individually because this lidar is a classical non-imaging lidar using two different APDs, one for each polarization channel.

The basic principle of depolarization ratio is similar as for the analysis of dual-image lidar data, however, since the dual-polarization lidar system only measured one spot of each target, and the polarization signals are already integrated signal, so we just simply use Eq. 5 to compute the linear depolarization ratio.

For most targets, two incident angles were measured. And since, for different targets, different attenuators were used, and we did not have access to those attenuation values, no reflectivity calculation is performed. The analysis results of depolarization ratios are shown in table 20.

***Table 20.*** *Depolarization ratios of solid targets at wavelength of 1.57 um*

| Target # | Linear Depolarization ratio, $\delta_L$ | | | | | | | | | | | |
|---|---|---|---|---|---|---|---|---|---|---|---|---|
| | Panel 1 | | Panel 2 | | Panel 3 | | Panel 4 | | Panel 5 | | Panel 6 | |
| | 0° | 15° | 0° | 15° | 0° | 15° | 0° | 15° | 0° | 15° | 0° | 15° |
| 4 | 0.48 | 0.48 | 0.21 | 0.38 | 0.01 | 0.07 | 0.07 | 0.46 | 0.43 | 0.45 | 0.04 | 0.08 |
| 5 | 0.36 | 0.47 | 0.25 | 0.33 | 0.02 | 0.04 | 0.08 | 0.21 | 0.47 | 0.36 | 0.41 | 0.34 |
| 6 | 0.57 | 0.57 | 0.32 | 0.36 | 0.08 | 0.18 | 0.47 | 0.45 | 0.47 | 0.48 | 0.39 | 0.73 |
| 7 | 0.74 | 0.73 | 0.26 | 0.42 | 0.03 | 0.16 | 0.40 | 0.46 | 0.09 | 0.08 | 0.09 | 0.10 |
| 8 | 0.39 | 0.40 | 0.36 | 0.40 | 0.01 | 0.05 | 0.50 | 0.51 | 0.45 | 0.46 | 0.56 | 0.69 |
| 9 | 0.31 | 0.28 | 0.35 | 0.45 | 0.05 | 0.22 | 0.40 | 0.37 | 0.16 | 0.18 | 0.37 | 0.45 |
| 10 | 0.37 | 0.53 | 0.44 | 0.47 | 0.01 | 0.05 | 0.20 | 0.14 | 0.22 | 0.17 | 0.28 | 0.53 |
| 11 | 0.09 | 0.23 | 0.39 | 0.53 | 0.02 | 0.07 | 0.23 | 0.14 | 0.43 | 0.41 | 0.34 | 0.52 |
| 12 | 0.81 | 0.50 | 0.24 | 0.35 | 0.04 | 0.08 | 0.48 | 0.19 | 0.41 | 0.42 | 0.40 | 0.37 |
| 13 | 0.05 | 0.14 | 0.23 | 0.25 | - | 0.04 | 0.06 | 0.09 | 0.02 | 0.06 | 0.05 | 0.09 |
| 14 | 0.44 | 0.42 | 0.33 | 0.18 | 0.02 | 0.10 | 0.10 | 0.09 | 0.08 | 0.31 | 0.39 | 0.34 |
| 15 | 0.66 | 0.52 | - | - | 0.14 | 0.15 | - | - | - | - | 0.08 | 0.16 |

Table 20 shows that at wavelength of 1570 nm, generally solid targets depolarization ratios increase when incident angle increases from 0° to 15° with a few exceptions. For some targets, it seems the incident angle influence over the depolarization ratios is little, and these targets usually have rough surfaces. Special targets are sand papers (panel 5) that their depolarization ratios at incident angle 0° and 15° are very close, except target #5 and #14 (actually, #14 is not sand paper). Figure 27 shows the depolarization ratios of solid targets on each panel and their change with incident angle.

In addition to the panel targets discussed above, at 1570 nm, we also examined different Spectralon reflectivity. The analysis results are shown in table 21.

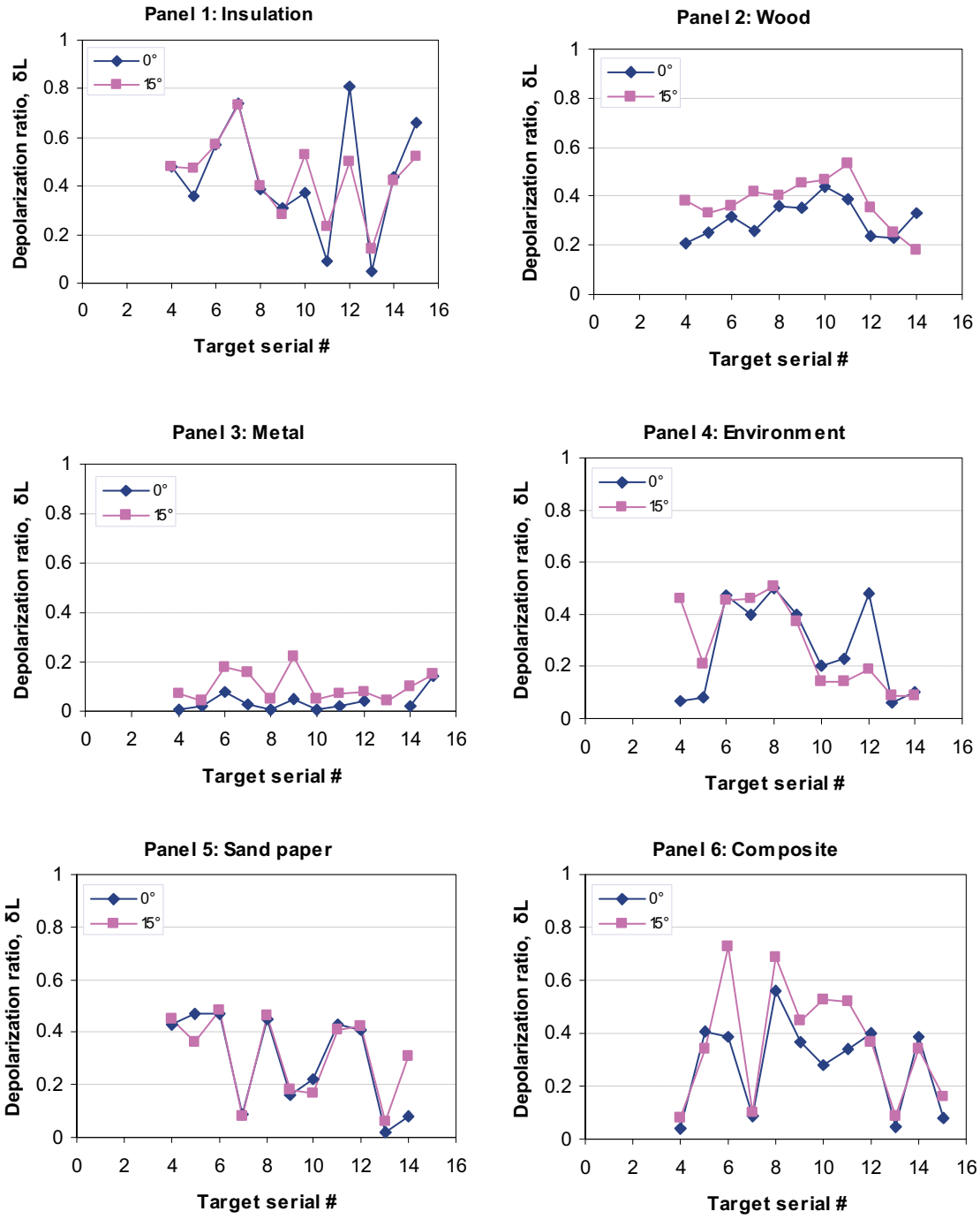


***Figure 27**. Depolarization ratio of solid targets and their change with incident angle at 1570 nm.*

Incident angle has little influence on Spectralon depolarization ratio.

***Table 21.*** *Depolarization ratios of Spectralons at wavelength of 1.57 um*

| *Serial #* | *Material* | L | | | |
|---|---|---|---|---|---|
| | | **0°** | **15°** | **30°** | **45°** |
| 1 | Spectralon: 2% | 0.07 | 0.10 | 0.10 | 0.12 |
| 2 | Spectralon: 50% | 0.48 | 0.45 | 0.51 | 0.49 |
| 3 | Spectralon: 75% | 0.47 | 0.52 | 0.48 | 0.53 |
| 4 | Spectralon: 99% | 0.50 | 0.57 | 0.49 | 0.52 |

# 6. Comparision of solid targets depolarization ratios at wavelength of 532 and 1570 nm

Now let's compare results from wavelengths of 532 nm and 1570 nm. Figure 28 shows the depolarization change at incident angle 0° and 15°, and at both wavelengths for targets on each panel.

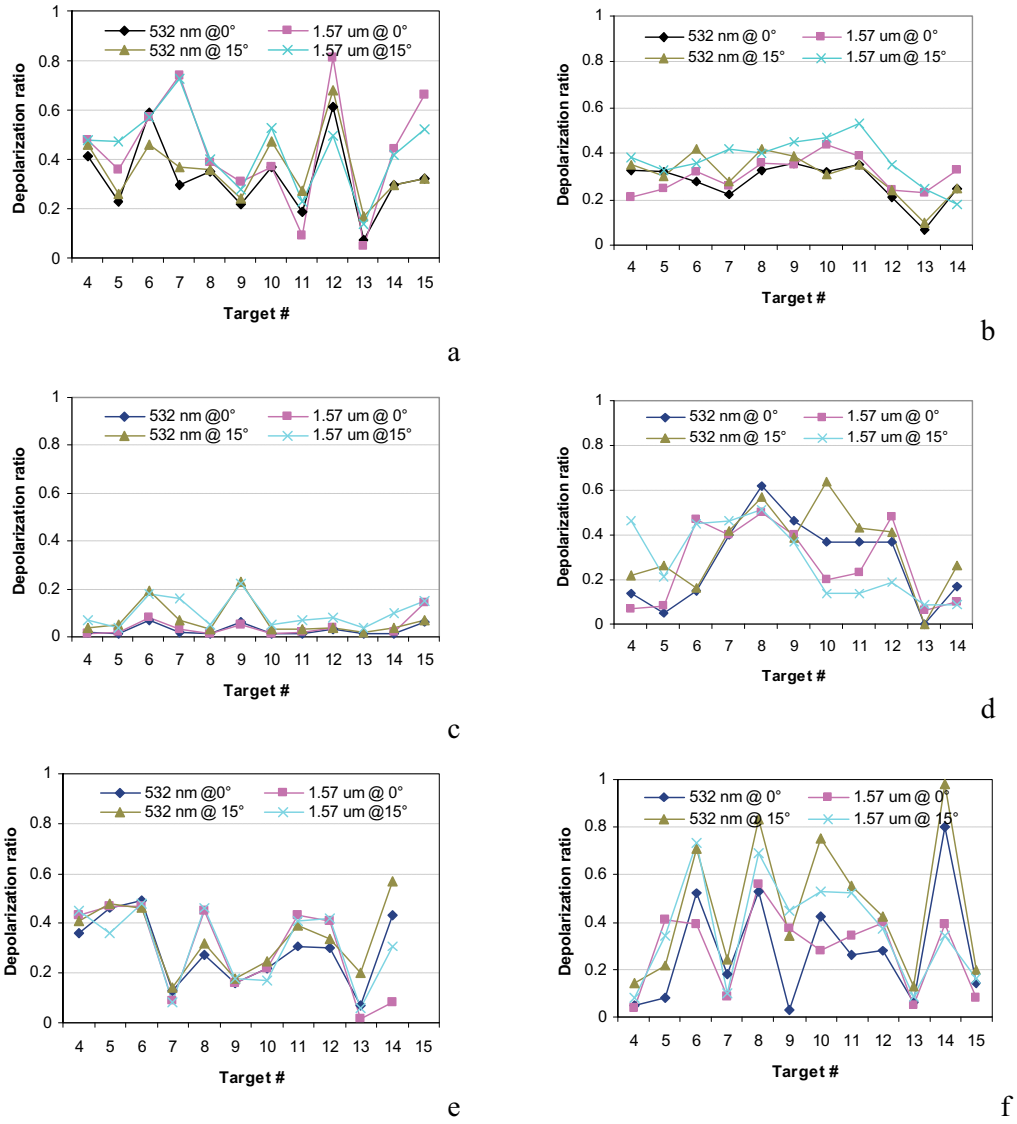


***Figure 28**. Depolarization ratio comparisn of solid targets between 532 and 1570 nm. (2) panel1, (b) panel 2, (c) panel 3, (d) panel 4, (e) panel 5 and (f) panel 6*

At both wavelengths, most solid targets depolarization ratios increase when incident angle increases from 0° to 15°, however, the change of sand papers are not as obvious as for other

targets. For wood targets, at wavelength of 532 nm, the incident angle influence to the depolarization ratio is very small. Generally, depolarization ratios of solid targets at 1570 nm are greater than those at 532 nm, however, it is not all the case for composite targets on panel 6, especially at incident angle 15°.

# 7. Conclusions and discussions

In this report, we have studied depolarization ratios and relative reflectivities for over 70 materials using an imaging polarization lidar operating at 532 nm and a dual polarization lidar operation at 1570nm. The major observations are as follow:

- Reflectivity of most targets decreases with light incident angle with exception of wood targets whose relative reflectivity seems to increase with incident angle.

- The depolarization ratio usually increases with incident angle, but sands, sand papers and grasses are exception, their depolarization ratio changing little with incident angle.

- Targets with high reflectivity usually showed higher depolarization ratios except metals which showed very high reflectivity at incident angle 0° but very low depolarization. The linear depolarization ratio approximately increases with reflectivity for diffusing material. Circular depolarization ratios are usually 2~3 times higher than their corresponding linear ones.

- Linear depolarization ratios of targets measured from lidar operating at 1.57 μm are usually higher than those from lidar operating at 532 nm. However, this is not quite true for targets with curved or very rough surfaces and uneven colors. These targets may show a trend totally opposite to above conclusions.

- Wavelength hardly affects the depolarization of most metals, and pretty similar for the influence of incident angle on depolarization ratios of sand papers. Among all the panel targets, metals are the worst depolarizers, showing depolarization ratios less than 0.05. Other targets, with low absorption, showed depolarization ratios ranging from 0.4 to 0.6.

Since two different lidar systems were used for wavelength of 532 and 1570 nm, lidar data collected were processed using different methods too. For the measurement using wavelength of 1.57 um lidar, each target was measured individually, thus fairly small divergent light beam was generated and the beam was fairly uniform. Very small part of each target was measured and used for the calculation of depolarization ratios. These two methods may not cause big change of the results for targets with smooth surface, but it is very possible to produce large difference when targets surface are very rough or have uneven colors, this could be remembered when doing results comparison between these two lidars.

The detection of target reflectivity greatly depends on the laser beam calibration (for 532 nm). Since the calibration was based on the average measurement of each pixel and the aerosols in

the air may not be always the same, the calibration is not perfect for each measurement, and sometimes relatively big errors may be induced.

To avoid the calibration errors induced by laser beam uniformity calibration, the best method appears to be to use a small divergent laser beam and measure each target individually, as was done when using the lidar at 1570 nm.

# 8. References


1. Kenneth Sassen, "Polarization in Lidar", chapter 2 in Lidar : *Range-Resolved Optical Remote Sensing of the Atmosphere*, Claus Weikamp Ed., Springer, New York. pp. 19-42 (2005).

2. Gilles Roy and Nathalie Roy. 'Relation between circular and linear depolarization ratios under multiple scattering conditions', Applied Optics, vol 47, pp.6563-6579 ( 2008)

3. Luc R Bissonnette, Gilles Roy and Grégoire Tremblay. 'Lidar-Based Characterization of the Geometry and Structure of Water Clouds'. Journal of atmospheric and ocean technology, Vol 24, pp 1364 –1376 (2007)

# List of symbols/abbreviations/acronyms/initialisms

| | |
|---|---|
| **DND** | **Department of National Defence** |
| **DRDC** | **Defense Research and Development Center** |
| **CCD** | **Charge Coupled Device** |
| **FOV** | **Field-of-View** |
| **G-ICCD** | **Gated-Intensified Charge Couples Device** |
| **ICCD** | **Intensified Charge Couples Device** |
| **LIDAR** | **Light Detection and Ranging** |
| **MFOV** | **Multiple-Field-of-View** |

## DOCUMENT CONTROL DATA

(Security classification of title, body of abstract and indexing annotation must be entered when the overall document is classified.)

1. ORIGINATOR (Name and address of the organization preparing the document.)

Daniel Pomerleau
AEREX avionique inc.
324, St- Augustin Ave.
Breakeyville, Québec, G0S 1E1

2. SECURITY CLASSIFICATION
(Overall security classification of the document, including special warning terms if applicable.)

UN

3. TITLE (The complete document title as indicated on the title page. Its classification should be indicated by the appropriate abbreviation (S, C or U) in parentheses after the title.)

Active polarimetric imaging of solid targets- Depolarization and reflectivity analysis

4. AUTHORS (Last name, followed by initials – ranks, titles, etc. not to be used.)

Xiaoying Cao

5. DATE OF PUBLICATION (month and year of publication of document.)

Novembre 2010

6. NO. OF PAGES (Including Annexes, Appendices and DCD sheet.)

43

7. DESCRIPTIVE NOTES (the category of the document, e.g. technical report, technical note or memorandum. If appropriate, enter the type of report, e.g. interim, progress, summary, annual or final. Give the inclusive dates when a specific reporting period is covered.)

Contractor Report

8a. PROJECT OR GRANT NO. (If appropriate, the applicable research and development project or grant number under which the document was written. Please specify whether project or grant)

8b. CONTRACT NO. (If appropriate, the applicable number under which the document was written)

W7701-072533

9a. ORIGINATOR'S DOCUMENT NUMBER (Official document number by which the document is identified by the originating activity. Number must be unique to this document.)

CR 2010-362

9b. OTHER DOCUMENT NOS. (Any other numbers which may be assigned to this document either by the originator or the sponsor.)

10. DOCUMENT AVAILABILITY (Any limitation on further distribution of the document, other than those imposed by security classification.)

( x ) Unlimited distribution
( ) Distribution limited to defence departments
( ) Distribution limited to defence contractors
( ) Distribution limited to government
( ) Distribution limited to Defence R&D Canada
( ) Controlled by Source

11. DOCUMENT ANNOUNCEMENT (Any limitation to the bibliographic announcement of this document. This will normally correspond to the Document Availability (10). However, where further distribution (beyond the audience specified in (10) is possible, a wider announcement audience may be selected.)

Unlimited

12. ABSTRACT (Brief and factual summary of the document. May also appear elsewhere in the body of the document itself. It is highly desirable that the abstract of classified documents be unclassified. Each paragraph of the abstract shall begin with an indication of the security classification of the information in the paragraph (unless the document itself is unclassified) represented as (S), (C), or (U). May be in English only).

Measurements of solid targets depolarization and reflectivity signatures were performed using a polarization imaging lidar. The lidar consists of a Q-switched laser operating at 532 nm, a telescope and a gated intensified CCD camera from Andor. Over 70 different materials have been examined. The different materials consist of different insulation materials, woods, metals, sand papers, concrete, wet/dry sands and environmental targets. Four incident angles measurements were conducted to examine the influence of light incident angle on the targets depolarization signature and reflectivity. The main observations are: (1) Metal targets show little depolarization but large reflectivity for incidence angle close to $0^{o}$; their reflectivity drops rapidly with an increase of the incident angle while depolarization increases. (2) Randomly oriented materials targets with high reflectivity show high depolarization ratio, and low reflectivity are associated with low depolarization ratio. Their depolarization ratios are almost not dependent on the light incident angle. (3) The circular depolarization ratios are typically 2 to 3 time larger than the linear depolarization ratios.

13. KEYWORDS, DESCRIPTORS or IDENTIFIERS (Technically meaningful terms or short phrases characterizing a document and could be helpful in cataloguing it. Should be **Unclassified** text. If not , the classification of each term should be indicated as with the title. Equipment model designation, trade name, military project code name, and geographic location may be included. If possible, should be selected from a published thesaurus. e.g. Thesaurus of Engineering and Scientific Terms (TEST) and that thesaurus-identified. )

Lidar, depolarization ratio, linear polarization, circular polarization

**Defence R&D Canada**

Canada's Leader in Defence
and National Security
Science and Technology

**R & D pour la défense Canada**

Chef de file au Canada en matière
de science et de technologie pour
la défense et la sécurité nationale

DEFENCE R&D DÉFENSE

**www.drdc-rddc.gc.ca**